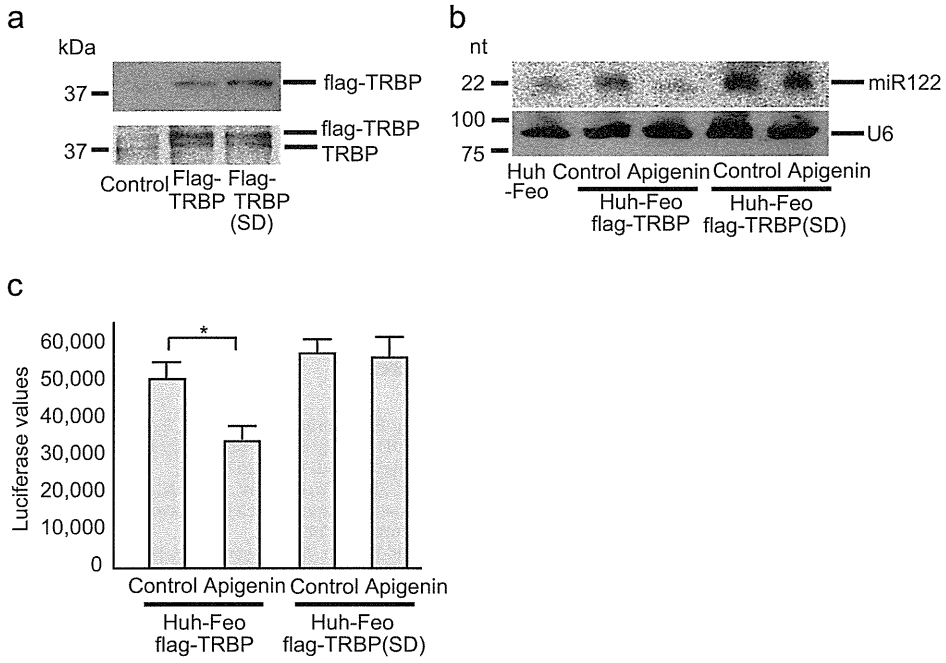

Fig. 3. Phosphorylation mimic TRBP blocks the inhibitory effects of apigenin on HCV replication. (a) Confirmation of flag-tagged TRBP-expressing construct expression. The expression of flag-tagged TRBP or phosphorylation mimic TRBP (TRBP(SD)) was confirmed by Western blotting using anti-flag and anti-TRBP antibodies. 293T cells were transiently transfected with constructs expressing the indicated proteins. Representative results from three independent experiments are shown. (b) TRBP (SD) blocked the inhibitory effects of apigenin on mature miR122 expression. Huh7-Feo cells were transduced with TRBP- or TRBP(SD)-expressing lentiviruses and selected. The expression levels of mature miR122 in Huh7-Feo cells, Huh7-Feo cells with TRBP expression, and Huh7-Feo cells with TRBP(SD) expression were determined by Northern blotting after 5 days of 5 μM apigenin treatment. U6 levels were used as a loading control. Representative results from three independent experiments are shown. (c) TRBP(SD) blocked the inhibitory effects of apigenin on HCV replication. Huh7-Feo cells with TRBP or TRBP(SD) expression were treated with 5 μM apigenin for 5 days and then subjected to luciferase assay. Data represent the means ± s.d. of the absolute luciferase values of three independent experiments. * $p < 0.05$.

conventional interferon, to eliminate HCV remains important. In addition, reducing miR122 expression may benefit patients with high cholesterol levels, because targeting miR122 with antisense oligonucleotides in vivo, including miravirsen in humans, decreases elevated cholesterol levels (Janssen et al., 2013). The effects of taking apigenin or eating foods rich in apigenin are worth considering.

Materials and methods

Cell culture

Huh7 and 293T cells were obtained from the Japanese Collection of Research Bioresources (JCRB, Osaka, Japan). Huh7-Feo cells that harbor an HCV replicon reporter construct (HCV-Feo) were kindly provided by Yokota et al. (2003). All cells were maintained in Dulbecco's modified Eagle's medium supplemented with 10% fetal bovine serum.

Reagents

Apigenin was purchased from Wako Chemicals (Osaka, Japan) and was dissolved in dimethyl sulfoxide (DMSO). Apigenin was added to the cell culture media at a 1:1000 dilution to reach the final working concentration. An equal volume of DMSO was used as a negative control.

Antibodies

Anti-luciferase antibody (#PM016) was purchased from MBL (Nagoya, Japan). Anti-β-actin antibody (#A5441), anti-flag M2 antibody (#F3165), and anti-TRBP antibody (SAB4200111) were purchased from Sigma (St. Louis, MO).

Western blotting, transfection, and dual luciferase assays

Western blotting, transfection, and dual luciferase assays were performed as we previously described (Kojima et al., 2011).

Quantitative RT-PCR analysis of miRNA expression

To determine miR122 and let-7g expression levels, cDNA was first synthesized from RNA, and quantitative PCR was then performed using the Mir-X miRNA First-Strand Synthesis and SYBR qRT-PCR Kit (Clontech, Mountain View, CA). miRNA precursor expression levels were determined according to a previous report (Suzuki et al., 2009) using the reported primers. Relative expression values were calculated by the CT-based calibrated standard curve method. These calculated values were then normalized to the expression of U6 snRNA. The reverse primer was provided in the kit.

Plasmids, viral production, and transduction

The firefly luciferase-based reporter carrying miR122-responsive elements in its 3′-UTR, which was used to examine miR122 function, and the internal control Renilla luciferase-based plasmids have been described previously (Kojima et al., 2011). A reporter with mutations in the miR122-responsive elements was constructed by inserting annealed oligonucleotides containing mutant miR122 binding sites downstream of the luciferase gene of pGL4. The oligonucleotide sequence used was CAA ACA CCA TTG TCA CAG CAG T. An HCV replicon expressing a chimeric protein consisting of firefly luciferase and neomycin phosphotransferase under the HCV 5′ IRES was used to monitor intracellular HCV replication levels (Yokota et al., 2003). To construct plasmids expressing wild-type TRBP or phosphorylation mimic TRBP (TRBP(SD)), flag-tagged TRBP cDNAs, amplified by PCR using plasmids containing cDNAs provided

by Paroo et al. (2009) as templates, were cloned into the pLVSIN vector (Takara, Shiga, Japan) at the *Not*1 site by a standard infusion method (Clontech).

Lentiviral production and transduction

Lentiviral particles carrying the flag-tagged TRBP-expressing constructs were produced using a pPACKH1 lentivector packaging plasmid mix according to the manufacturers' recommendations (System Biosciences). Huh7-Feo cells were transduced with lentiviruses using polybrene (EMD Millipore, Billerica, MA, USA), and were then selected with puromycin (6 μg/ml).

Northern blotting of miRNAs

Northern blotting of miRNAs was performed as described previously (Takata et al., 2013b). Briefly, total RNA was extracted using TRIzol Reagent (Invitrogen, Carlsbad, CA) according to the manufacturer's instructions. 10 mg of RNA were resolved in denaturing 15% polyacrylamide gels containing 7 M urea in 1 × TBE and then transferred to a Hybond N+ membrane (GE Healthcare) in 0.25 × TBE. Membranes were UV-crosslinked and prehybridized in hybridization buffer. Hybridization was performed overnight at 42 °C in ULTRAhyb-Oligo Buffer (Ambion) containing a biotinylated probe specific for miR122 (CAA ACA CCA TTG TCA CAC TCC A) that had been heated to 95 °C for 2 min. Membranes were washed at 42 °C in 2 × SSC containing 0.1% SDS, and the bound probe was visualized using a BrightStar BioDetect Kit (Ambion). Blots were stripped by boiling in a solution containing 0.1% SDS and 5 mM EDTA for 10 min prior to rehybridization with a U6 probe (CAC GAA TTT GCG TGT CAT CCT T).

Cell counting

Relative cell proliferation was assessed using Cell Counting Kit-8 (Dojindo Laboratories), as we previously described (Kojima et al., 2011).

Synthesized miRNAs and transfection

Synthesized anti-miR122 oligonucleotides, mature miRNA122, and let7g mimics were purchased from Sigma and were transiently transfected at a final concentration of 10 pM using RNAi Max Reagent according to the manufacturer's instructions (Sigma).

Statistical analysis

When the variances were equal, statistically significant differences between groups were identified using Student's *t*-test. When the variances were unequal, Welch's *t*-test was used instead. P values <0.05 were considered to indicate statistical significance in in vitro experiments.

Author contributions

C.S. and M.Otsuka planned the research and wrote the manuscript. C.S., M.Ohno, T.K., T.Y. and A.T. performed the majority of the experiments. K.G., R.M., and N.K. provided materials and supported some parts of experiments. C.S., M.Ohno and M.Otsuka analyzed the data. K.K. supervised the entire project.

Acknowledgments

This work was supported by Grants-in-Aid from the Ministry of Education, Culture, Sports, Science and Technology, Japan (# 25293076, #25860520, and #24390183) (to M.O., T.Y., K.K.), by Health Sciences Research Grants of The Ministry of Health, Labour and Welfare of Japan (to K.K.), by a grant from the Mishima Kaiun Memorial Foundation (to M. Ohno), and by grants from the Honjo International Scholarship Foundation and the Japanese Society of Gastroenterology (to M.O.).

References

Bacon, B.R., Gordon, S.C., Lawitz, E., Marcellin, P., Vierling, J.M., Zeuzem, S., et al., 2011. Boceprevir for previously treated chronic HCV genotype 1 infection. New Engl. J. Med. 364, 1207–1217.

Cao, J., Zhang, Y., Chen, W., Zhao, X., 2010. The relationship between fasting plasma concentrations of selected flavonoids and their ordinary dietary intake. Br. J. Nutr. 103, 249–255.

Deuffic-Burban, S., Schwarzinger, M., Obach, D., Mallet, V., Pol, S., Pageaux, G.P., et al., 2014. Should we await IFN-free regimens to treat HCV genotype 1 treatment-naive patients? A cost-effectiveness analysis (ANRS 12188). J. Hepatol, in press.

Elmén, J., Lindow, M., Schütz, S., Lawrence, M., Petri, A., Obad, S., et al., 2008. LNA-mediated microRNA silencing in non-human primates. Nature 452, 896–899.

Gebert, L.F., Rebhan, M.A., Crivelli, S.E., Denzler, R., Stoffel, M., Hall, J., 2014. Miravirsen (SPC3649) can inhibit the biogenesis of miR-122. Nucleic Acids Res. 42, 609–621.

Gramantieri, L., Ferracin, M., Fornari, F., Veronese, A., Sabbioni, S., Liu, C.G., et al., 2007. Cyclin G1 is a target of miR-122a, a microRNA frequently down-regulated in human hepatocellular carcinoma. Cancer Res. 67, 6092–6099.

Hou, J., Lin, L., Zhou, W., Wang, Z., Ding, G., Dong, Q., et al., 2011. Identification of miRNomes in human liver and hepatocellular carcinoma reveals miR-199a/b-3p as therapeutic target for hepatocellular carcinoma. Cancer Cell 19, 232–243.

Hsu, S.H., Wang, B., Kota, J., Yu, J., Costinean, S., Kutay, H., et al., 2012. Essential metabolic, anti-inflammatory, and anti-tumorigenic functions of miR-122 in liver. J. Clin. Investig. 122, 2871–2883.

Jacobson, I.M., McHutchison, J.G., Dusheiko, G., Di Bisceglie, A.M., Reddy, K.R., Bzowej, N.H., et al., 2011. Telaprevir for previously untreated chronic hepatitis C virus infection. New Engl. J. Med. 364, 2405–2416.

Janssen, H.L., Reesink, H.W., Lawitz, E.J., Zeuzem, S., Rodriguez-Torres, M., Patel, K., et al., 2013. Treatment of HCV infection by targeting MicroRNA. New Engl. J. Med 368, 1685–1694.

Jopling, C., 2012. Liver-specific microRNA-122: biogenesis and function. RNA Biol. 9, 137–142.

Jopling, C.L., Yi, M., Lancaster, A.M., Lemon, S.M., Sarnow, P., 2005. Modulation of hepatitis C virus RNA abundance by a liver-specific MicroRNA. Science 309, 1577–1581.

Kojima, K., Takata, A., Vadnais, C., Otsuka, M., Yoshikawa, T., Akanuma, M., et al., 2011. MicroRNA122 is a key regulator of α-fetoprotein expression and influences the aggressiveness of hepatocellular carcinoma. Nat. Commun. 2, 338.

Krützfeldt, J., Rajewsky, N., Braich, R., Rajeev, K.G., Tuschl, T., Manoharan, M., et al., 2005. Silencing of microRNAs in vivo with 'antagomirs'. Nature 438, 685–689.

Kutay, H., Bai, S., Datta, J., Motiwala, T., Pogribny, I., Frankel, W., et al., 2006. Downregulation of miR-122 in the rodent and human hepatocellular carcinomas. J. Cell. Biochem. 99, 671–678.

Lanford, R.E., Hildebrandt-Eriksen, E.S., Petri, A., Persson, R., Lindow, M., Munk, M. E., et al., 2010. Therapeutic silencing of microRNA-122 in primates with chronic hepatitis C virus infection. Science 327, 198–201.

Li, Y.P., Gottwein, J.M., Scheel, T.K., Jensen, T.B., Bukh, J., 2011. MicroRNA-122 antagonism against hepatitis C virus genotypes 1-6 and reduced efficacy by host RNA insertion or mutations in the HCV 5′ UTR. Proc. Natl. Acad. Sci. U.S.A. 108, 4991–4996.

Manns, M.P., von Hahn, T., 2013. Novel therapies for hepatitis C—one pill fits all? Nat. Rev. Drug Discov. 12, 595–610.

Ohno, M., Shibata, C., Kishikawa, T., Yoshikawa, T., Takata, A., Kojima, K., et al., 2013. The flavonoid apigenin improves glucose tolerance through inhibition of microRNA maturation in miRNA103 transgenic mice. Sci. Rep. 3, 2553.

Otsuka, M., Kishikawa, T., Yoshikawa, T., Ohno, M., Takata, A., Shibata, C., et al., 2014. The role of microRNAs in hepatocarcinogenesis: current knowledge and future prospects. J. Gastroenterol. 49, 173–184.

Paroo, Z., Ye, X., Chen, S., Liu, Q., 2009. Phosphorylation of the human microRNA-generating complex mediates MAPK/Erk signaling. Cell 139, 112–122.

Pfeffer, S., Baumert, T.F., 2010. Impact of microRNAs for pathogenesis and treatment of hepatitis C virus infection. Gastroenterol. Clin. Biol. 34, 431–435.

Poordad, F., McCone, J., Bacon, B.R., Bruno, S., Manns, M.P., Sulkowski, M.S., et al., 2011. Boceprevir for untreated chronic HCV genotype 1 infection. New Engl. J. Med. 364, 1195–1206.

Scheel, T.K., Rice, C.M., 2013. Understanding the hepatitis C virus life cycle paves the way for highly effective therapies. Nat. Med. 19, 837–849.

Sherman, K.E., Flamm, S.L., Afdhal, N.H., Nelson, D.R., Sulkowski, M.S., Everson, G.T., et al., 2011. Response-guided telaprevir combination treatment for hepatitis C virus infection. New Engl. J. Med. 365, 1014–1024.
Snyder, S.A., Gollner, A., Chiriac, M.I., 2011. Regioselective reactions for programmable resveratrol oligomer synthesis. Nature 474, 461–466.
Suzuki, H.I., Yamagata, K., Sugimoto, K., Iwamoto, T., Kato, S., Miyazono, K., 2009. Modulation of microRNA processing by p53. Nature 460, 529–533.
Takata, A., Otsuka, M., Yoshikawa, T., Kishikawa, T., Ohno, M., Koike, K., 2013a. MicroRNAs and liver function. Minerva Gastroenterol. Dietol. 59, 187–203.
Takata, A., Otsuka, M., Yoshikawa, T., Kishikawa, T., Hikiba, Y., Obi, S., et al., 2013b. MicroRNA-140 acts as a liver tumor suppressor by controlling NF-κB activity by directly targeting DNA methyltransferase 1 (Dnmt1) expression. Hepatology 57, 162–170.
Tsai, W.C., Hsu, P.W., Lai, T.C., Chau, GY, Lin, CW, Chen, CM, et al., 2009. MicroRNA-122, a tumor suppressor microRNA that regulates intrahepatic metastasis of hepatocellular carcinoma. Hepatology 49, 1571–1582.
Tsai, W.C., Hsu, S.D., Hsu, C.S., Lai, T.C., Chen, S.J., Shen, R., et al., 2012. MicroRNA-122 plays a critical role in liver homeostasis and hepatocarcinogenesis. J. Clin. Investig. 122, 2884–2897.
Yokota, T., Sakamoto, N., Enomoto, N., Tanabe, Y., Miyagishi, M., Maekawa, S., et al., 2003. Inhibition of intracellular hepatitis C virus replication by synthetic and vector-derived small interfering RNAs. EMBO Rep. 4, 602–608.

Clinica Chimica Acta 433 (2014) 128–134

Contents lists available at ScienceDirect

Clinica Chimica Acta

journal homepage: www.elsevier.com/locate/clinchim

Increased serum autotaxin levels in hepatocellular carcinoma patients were caused by background liver fibrosis but not by carcinoma

Mayuko Kondo [a], Takeaki Ishizawa [c], Kenichiro Enooku [a,b], Yasunori Tokuhara [b], Ryunosuke Ohkawa [b], Baasanjav Uranbileg [b], Hayato Nakagawa [a], Ryosuke Tateishi [a], Haruhiko Yoshida [a], Norihiro Kokudo [c], Kazuhiko Koike [a], Yutaka Yatomi [b], Hitoshi Ikeda [a,b,*]

[a] Department of Gastroenterology, Graduate School of Medicine, The University of Tokyo, Tokyo, Japan
[b] Department of Clinical Laboratory Medicine, Graduate School of Medicine, The University of Tokyo, Tokyo, Japan
[c] Hepato–Biliary–Pancreatic Surgery Division, Department of Surgery, Graduate School of Medicine, The University of Tokyo, Tokyo, Japan

ARTICLE INFO

Article history:
Received 27 December 2013
Received in revised form 26 February 2014
Accepted 10 March 2014
Available online 16 March 2014

Keywords:
Autotaxin
Hepatocellular carcinoma
Lysophosphatidic acid
Liver fibrosis

ABSTRACT

Background: Controversy exists as to whether autotaxin (ATX) may be importantly associated with pathophysiology of hepatocellular carcinoma (HCC).
Methods: We evaluated serum ATX levels and its mRNA expression in consecutive 148 HCC patients treated with radiofrequency ablation (RFA) and 30 patients with hepatic resection.
Results: Although increased serum ATX levels were observed in almost all the patients treated with RFA, they were not reduced after RFA. Furthermore, serum ATX levels were associated not with tumor burden but with the parameters predicting for liver fibrosis, such as liver stiffness values. Then, in surgically-treated patients, there was no significant correlation between serum ATX levels and ATX mRNA expression levels in HCC tissues. Notably, ATX mRNA expression levels in HCC tissues were not higher than those in peri-tumorous tissues. Finally, serum ATX levels in surgically-treated HCC patients were rather correlated with ATX mRNA expression levels in peri-tumorous tissues as well as with liver fibrosis stage.
Conclusion: The increase in serum ATX levels in HCC patients may not be caused by abundant ATX production in HCC tissues but by fibrosis in the background livers.

1. Introduction

Because ATX was originally discovered in a conditioned medium from human melanoma cell cultures as a stimulator of cell migration [1], ATX has long been speculated to play a role in cancer invasion or metastasis as an autocrine motility factor [2]. Indeed, a potential role of ATX in cancer pathophysiology has been intensively studied; enhanced ATX expression has been reported in Hodgkin lymphoma [3], glioblastoma [4], non-small cell lung cancer [5], renal cell carcinoma [6], breast cancer [7], thyroid carcinoma [8] as well as melanoma [2].

The pathophysiological significance of ATX has been unveiled by the finding that ATX possesses lysophospholipase D activity [9,10], hydrolyzing lysophosphatidylcholine to produce lysophosphatidic acid (LPA), a lipid mediator, eliciting a wide variety of biological responses including cell migration, neurogenesis, angiogenesis, smooth-muscle contractions, platelet aggregation, and wound healing [11]. The pathophysiological functions of ATX are now assumed to be largely attributable to the ability of ATX to produce LPA. Of note, ATX is responsible for producing LPA in the blood by hydrolysis of lysophospholipids (mainly lysophosphatidylcholine) [12]. In fact, in the plasma from heterozygous ATX-null mice, LPA levels were about half those in the plasma from wild-type mice [13], and a strong correlation between serum ATX activity and plasma LPA levels has also been observed in humans [14] and rats [15], suggesting that serum ATX activity may be one of the key determinants of plasma LPA levels.

There has been evidence showing the overexpression of ATX in HCC [16–19]. Furthermore, this increased ATX expression in HCC reportedly led to abundant tumor-secreted LPA, and as a result serum LPA levels were higher in HCC patients with more tumor burden, i.e., with metastasis than in those without [18]. In contrast, there has been a report, showing no correlation between plasma LPA levels and the tumor burden of HCC [20]. Thus, controversy exists as to whether ATX and LPA are importantly associated with HCC pathophysiology. To clarify this, serum ATX levels were analyzed in HCC patients who underwent radiofrequency ablation (RFA) or hepatic resection in consideration of tumor burden, treatment effects and ATX mRNA expression in HCC tissues.

Abbreviations: ATX, autotaxin; HCC, hepatocellular carcinoma; RFA, radiofrequency ablation; LPA, lysophosphatidic acid; APRI, aspartate aminotransferase-to-platelet ratio index.

* Corresponding author at: Department of Clinical Laboratory Medicine, Graduate School of Medicine, The University of Tokyo, 7-3-1 Hongo, Bunkyo-ku, Tokyo 113-8655, Japan. Tel.: +81 3 3815 5411; fax: +81 3 5689 0495.
E-mail address: ikeda-1im@h.u-tokyo.ac.jp (H. Ikeda).

http://dx.doi.org/10.1016/j.cca.2014.03.006
0009-8981/

2. Patients and methods

2.1. Patients

We enrolled 148 consecutive patients with HCC who underwent RFA between November 2012 and March 2013 at the Department of Gastroenterology, and 30 consecutive patients with HCC who underwent hepatic resection between January 2013 and June 2013 at the Hepato-Biliary–Pancreatic Surgery Division, the Department of Surgery, the University of Tokyo Hospital, Tokyo, Japan. HCC was diagnosed as previously described [21]. Patients with HCC recurrence as well as those with the first occurrence were included in this study.

This study was carried out in accordance with the ethical guidelines of the 1975 Declaration of Helsinki and was approved by the Institutional Research Ethics Committee of the Faculty of Medicine of the University of Tokyo. Informed consent from the patients was obtained for the use of all the samples.

2.2. RFA

The detailed procedure of RFA using a cooled-tip electrode (Covidien) was meticulously described elsewhere [22,23]. In general, we performed RFA on Child-Pugh class A or B patients, a single tumor ≤5 cm in diameter, or ≤3 tumors ≤3 cm in diameter. Treatment efficacy was evaluated by dynamic CT performed 1 to 3 days post-ablation. In the case of incomplete ablation, patients underwent additional ablation sessions until complete tumor coverage was achieved.

2.3. Evaluation of tumor volume

We estimated the volume of each HCC lesion as the sphere taking the greatest axial dimension as the diameter in our present analyses.

2.4. Measurement of ATX antigen

Serum ATX antigen level was determined in all enrolled patients 1 day to 1 week prior to the treatment using a specific 2-site enzyme immunoassay, as previously described, in which the within-run and between-run CVs were 3.1–4.6% and 2.8–4.6%, respectively [24]. In 90 patients, serum ATX antigen level was also measured 2 to 4 weeks after RFA.

2.5. Measurement of liver stiffness

Liver stiffness was measured using transient elastography (FibroScan 502; EchoSens), as described previously [25]. Patients were without active liver damage with >100 U/l of alanine aminotransferase (ALT) and cardiac insufficiency, because liver stiffness value has been shown to be unreliable to predict the degree of liver fibrosis in those conditions [26,27].

2.6. Quantitative real time PCR

Total RNA of HCC and peri-tumorous tissues was extracted using TRIZOL reagent (Invitrogen). One microgram of purified total RNA was transcribed using SuperScript™ First-Strand Synthesis System for RT-PCR (Invitrogen). Quantitative real time PCR was performed with SYBR green PCR Master Mix (Applied Biosystems Inc.) with primers specific for ATX and beta-actin designed by NCBI Primer Designing Tool. The primer pairs were used as follows: human ATX (NM_006209.4): 5′-CGTGGCTGGGAGTGTACTAA-3′ and 5′-AGAGTGTGTGCCACAAGACC-3′, human beta-actin (NM_001101.3): 5′-GGGTCAGAAGGATTCCTATG-3′ and 5′-CCTTAATGTCACGCACGATTT-3′. The PCR reaction was performed in a volume of 25 μl containing 1 μl of cDNA, 12.5 μl of SYBR Green Master Mix. PCR amplifications were run using the following conditions: 10 min at 95 °C, followed by 40 cycles of 15 s at 95 °C and 1 min at 60 °C. The target gene mRNA expression level was relatively quantified to beta-actin using $2^{-\Delta\Delta Ct}$ method (Applied Biosystems, User Bulletin No. 2).

2.7. Histological staging

Fibrosis stage, determined according to the METAVIR group scoring system, was classified as F0, no fibrosis; F1, portal fibrosis without septa; F2, few septa; F3, numerous septa without cirrhosis; or F4, cirrhosis.

2.8. Statistical analysis

The Wilcoxon signed-rank test was used when comparing 2 matched samples (before and after RFA) to assess whether their population mean ranks differ. The Wilcoxon rank-sum test was used to determine whether 2 groups of data are different. Correlations were determined using the Spearman's rank correlation coefficient. The association between ATX mRNA expression in peri-tumorous tissues and fibrosis stage was assessed with the Jonckeere–Terpstra test. A 2-sided $P < 0.05$ was considered statistically significant. All statistical analyses were performed using R 2.13.0 (http://www.R-project.org).

3. Results

3.1. Characteristics of patients who underwent RFA

The characteristics of the enrolled patients who underwent RFA are shown in Table 1. The median age was 72.4 y, in agreement with the notion that HCC patients in Japan have been getting old [28]. Male and

Table 1
Characteristics of patients who underwent RFA.

Variable	$n = 148$
Age (y)	72.4 (65.6–78.9)
Sex, *n* (%)	
Male	105 (70.9)
Female	43 (29.1)
Viral markers, *n* (%)	
HBsAg, positive	19 (12.8)
Anti-HCVAb, positive	107 (72.3)
Both positive	1 (0.7)
Both negative	21 (14.2)
AST (U/l)	44.0 (31.8–66.3)
ALT (U/l)	35.0 (20.8–54.0)
Albumin (g/dl)	3.5 (3.1–3.9)
Platelet count ($\times 10^9$/l)	112 (74–152)
Child Pugh classification	
Class A	119 (80.4)
Class B	28 (18.9)
Class C	1 (0.7)
Size of main tumor (cm)	1.5 (1.1–2.0)
No. of tumors	
1	97 (65.5)
2	31 (20.9)
3	14 (9.5)
4	2 (1.4)
5	4 (2.7)
Total volume of tumors (cm^3)	2.5 (0.9–4.2)
Serum ATX level (mg/l) in total	2.21 ± 1.03
In male	1.94 ± 1.01
In female	2.87 ± 0.76
AFP (ng/ml)	11.9 (4.9–35.1)
	$n = 101$
Fibroscan (kPa)	22.3 (12.9–35.8)
Serum hyaluronic acid level (mg/l)	272.8 (129.1–507.7)
Serum type IV collagen 7S (ng/ml)	6.4 (4.7–8.3)

Values are expressed as median and range (25th–75th percentiles), mean ± SD, or number (percent). Abbreviations: HBsAg, hepatitis B surface antigen; anti-HCVAb, antihepatitis C virus antibody.

HCV-infected patients were predominant. The median liver stiffness values and serum hyaluronic levels were 22.3 kPa and 272.8 mg/l, respectively, suggesting that a major part of patients had advanced liver fibrosis.

Because serum ATX levels have gender differences [29], which are higher in women than in men, serum ATX levels were analyzed in men and women, respectively. Serum ATX levels in the studied patients, 1.94 ± 1.01 mg/l (mean ± SD) in male and 2.87 ± 0.76 mg/l in female patients, were increased and above the central 95 percentile reference interval of healthy controls [24], in 94 of 105 (89.5%) male patients and in all female patients (Fig. 1A). These values are not higher than those in patients with chronic liver disease caused by hepatitis C virus (C-CLD) in the absence of HCC in a previous cohort, which were 2.07 ± 0.81 mg/l in male patients (n = 42) and 2.85 ± 0.97 mg/l in female patients (n = 32) [30]. When we focused on patients with liver cirrhosis caused by C-CLD, serum ATX levels were 2.48 ± 0.74 mg/l in male patients (n = 16) and 3.20 ± 0.93 mg/l in female patients (n = 20), where the former was significantly higher than those in male HCC patients ($P = 6.6 \times 10^{-3}$, Wilcoxon rank-sum test). These results suggest that serum ATX levels in HCC patients were not higher than those in patients with C-CLD, and they were rather lower than those in patients with liver cirrhosis. On the other hand, serum alpha-fetoprotein (AFP) levels were above the upper limit of the normal range in our hospital (>9 ng/ml) in 82 of 148 (55.4%) patients.

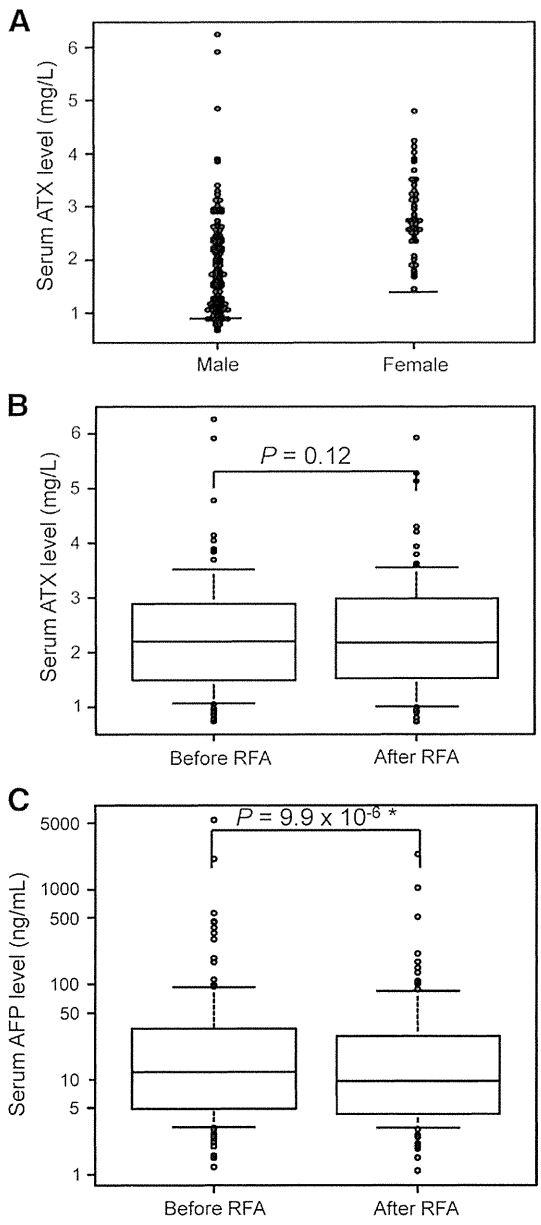

Fig. 1. Serum ATX and AFP levels in HCC patients treated with RFA. (A) Serum ATX levels in 148 HCC patients treated with RFA. The horizontal bars indicate the upper limit of 95 percentile reference interval for the healthy controls. (B) Serum ATX levels in HCC patients (63 males and 27 females) before and after RFA. (C) Serum AFP levels in HCC patients (90 males and 36 females) before and after RFA. The differences of serum ATX and AFP levels before and after RFA were analyzed by using Wilcoxon signed-rank test. The asterisk indicates the significant difference.

3.2. Serum ATX levels in patients with HCC before and after RFA

To examine a potential relationship between serum ATX levels and HCC, serum ATX levels were measured before and after RFA (2 to 4 weeks) in 90 patients (63 male and 27 female patients). Serum AFP levels were also measured before and after RFA in 126 patients. As a result, serum ATX levels were 2.30 ± 1.08 mg/l before RFA, and 2.32 ± 1.06 mg/l after RFA, which were essentially unaltered as shown in Fig. 1B ($P = 0.12$). Then, we compared serum ATX levels before and after RFA in two patient groups, the patients whose samples were collected 2 to 3 weeks after RFA (n = 61) and those whose samples were collected 3 to 4 weeks after RFA (n = 29). The changes in serum ATX levels before and after RFA were 0.034 ± 0.262 mg/l in the former group, and −0.007 ± 0.503 mg/l in the latter group, which were essentially unaltered ($P = 0.99$, Wilcoxon rank-sum test). In contrast, a substantial decrease was observed after complete ablation in serum AFP levels ($P = 9.9 \times 10^{-6}$), as shown in Fig. 1C. Collectively, the treatment of HCC with RFA led to a decrease in serum AFP levels but not in serum ATX levels.

3.3. Relationship between serum ATX levels and tumor burden

We then examined whether serum ATX levels might be associated with tumor burden. Fig. 2 depicts that there was no significant correlation between serum ATX levels and the maximum diameter of HCC both in men and women (Fig. 2A & B). When total volume was employed for the evaluation of tumor burden of HCC, there was similarly no significant correlation between serum ATX levels and the total volume of HCC both in men and women (Fig. 2C & D). Collectively, there was no association between serum ATX levels and tumor burden.

3.4. Relationships between serum ATX levels and other parameters

The parameters related to liver functions were analyzed whether they might correlate with serum ATX levels. The strong correlations were observed between serum ATX levels and the parameters predicting for liver fibrosis, i.e., liver stiffness values, serum hyaluronic acid levels, serum type IV collagen 7S levels, and aspartate aminotransferase-to-platelet ratio index (APRI) as shown in Fig. 2E, F and Table 2. These results may be in line with the previous finding that serum ATX levels were correlated with the stage of liver fibrosis in patients with chronic hepatitis C [14,30]. The significant correlations were also observed between serum ATX levels and the parameters related to liver functions such as serum albumin levels, serum total bilirubin levels, serum aspartate aminotransferase (AST) and alanine aminotransferase (ALT) levels, serum alkaline phosphatase (ALP) levels and serum AFP levels. These results suggest that the increase in serum ATX levels in patients with HCC may be associated with fibrosis in the background liver bearing HCC.

3.5. Characteristics of patients who underwent hepatic resection

Then, we could directly examine ATX mRNA expression in HCC tissues in patients who underwent hepatic resection. The characteristics of the enrolled patients are shown in Table 3. There were a higher

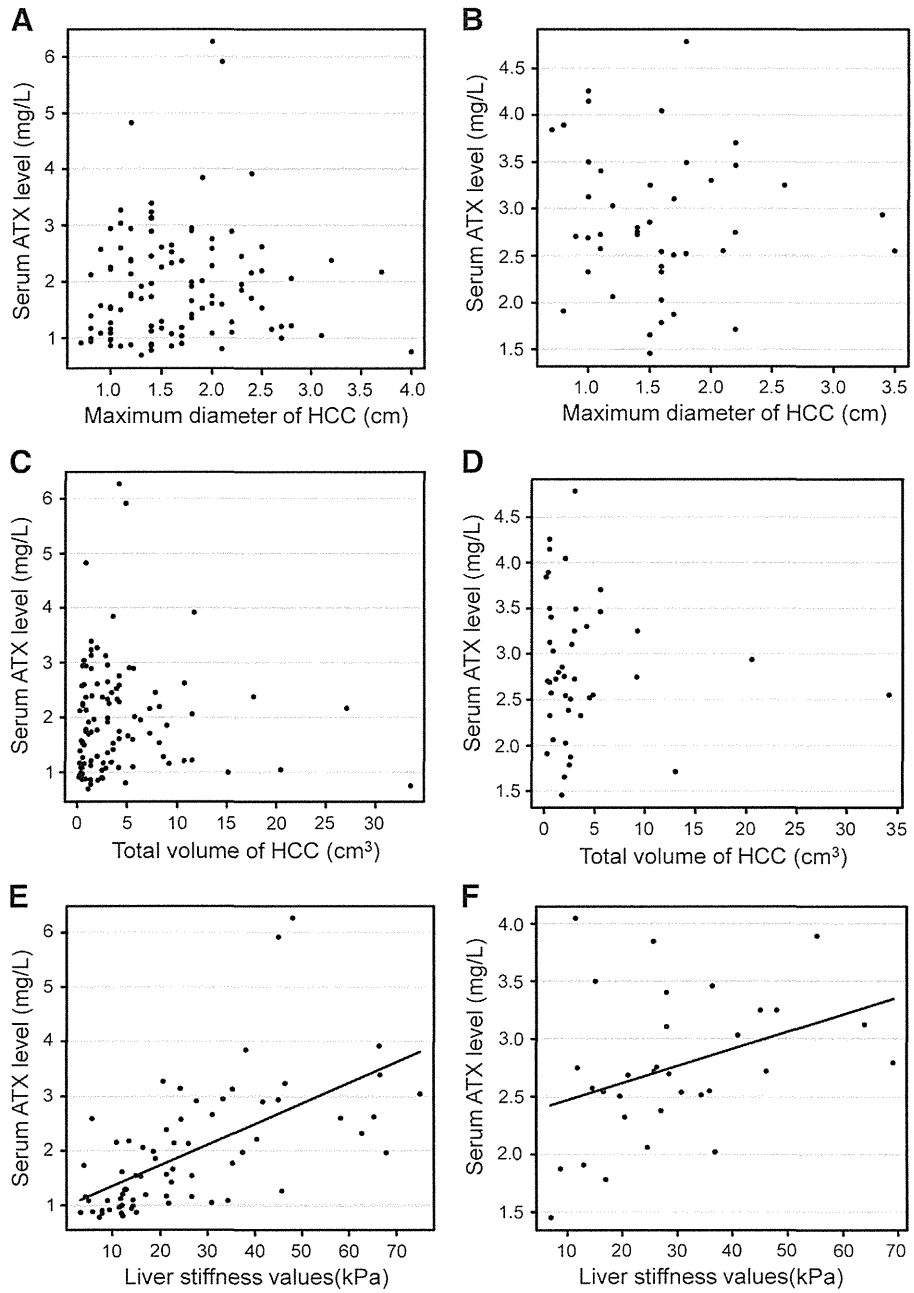

Fig. 2. Relationship between serum ATX levels and HCC burden or liver stiffness in HCC patients. Relationships between serum ATX levels and the maximum diameter of HCC in male (A) and female (B) patients, or total volume of HCC in male (C) and female (D) patients are shown. Data from 148 HCC patients (105 males and 43 females) treated with RFA were used to analyze a relationship by using Spearman's rank correlation coefficient. No significant correlation was observed between serum ATX levels and the maximum diameter (Spearman's rank correlation coefficient; $\rho = 0.11$, $P = 0.25$ (A) and $\rho = -0.096$, $P = 0.54$ (B)) or total volume of nodules (Spearman's rank correlation coefficient; $\rho = 0.14$, $P = 0.14$ (C) and $\rho = -0.091$, $P = 0.56$ (D)). Then, relationships between serum ATX levels and liver stiffness values in male (E) and female (F) HCC patients are shown. Data from 101 HCC patients (69 males and 32 females) treated with RFA were used to analyze a relationship by using Spearman's rank correlation coefficient. A significant correlation was observed between serum ATX levels and liver stiffness values (Spearman's rank correlation coefficient; $\rho = 0.70$, $P = 3.0 \times 10^{-11}$ (E) and $\rho = 0.40$, $P = 0.025$ (F)).

proportion of patients who had neither hepatitis B surface antigen nor anti-hepatitis C virus antibody in patients who underwent hepatic resection compared to those who underwent RFA. Patients who underwent hepatic resection had more platelet counts and less serum ATX levels, suggesting that the fibrosis in the background liver may be less severe.

3.6. ATX mRNA expression levels in HCC and peri-tumorous tissues

We investigated ATX mRNA expression levels in HCC tissues and in peri-tumorous tissues. As depicted in Fig. 3A, ATX mRNA expression levels in HCC tissues were not higher than those in peri-tumorous tissues; ATX mRNA expression was higher in tumorous tissues than in peri-tumorous tissues in 8 out of 30 patients (Fig. 3B). When examining a relationship to serum ATX levels, there was no significant correlation between ATX mRNA expression levels in HCC tissues and serum ATX levels, as shown in Fig. 3C (Spearman's rank correlation coefficient; $\rho = 0.14$, $P = 0.50$, $n = 26$), suggesting that ATX mRNA expression in HCC tissues may not contribute to the increase in serum ATX levels in HCC patients.

On the other hand, a significant correlation was observed between serum ATX levels and ATX mRNA expression levels in peri-tumorous tissues, as depicted in Fig. 3D (Spearman's rank correlation coefficient; $\rho = 0.50$, $P = 9.8 \times 10^{-3}$). Furthermore, ATX mRNA expression levels

Table 2
Correlation of serum ATX levels with other parameters in HCC patients treated with RFA in 105 male and 43 female patients.

	ρ	P		ρ	P
Male patients					
Albumin (g/dl)	−0.63	7.5×10^{-13}	Platelet count ($\times 10^9$/l)	−0.53	5.6×10^{-9}
Total bilirubin (mg/dl)	0.40	2.8×10^{-5}	Liver stiffness values (kPa)	0.70	3.5×10^{-11}
AST (U/l)	0.69	6.1×10^{-16}	APRI	0.71	$<2.2 \times 10^{-16}$
ALT (U/l)	0.53	5.6×10^{-9}	Hyaluronic acid (mg/l)	0.67	$<2.2 \times 10^{-16}$
ALP (U/l)	0.65	4.3×10^{-14}	Type IV collagen 7S (ng/ml)	0.79	3.7×10^{-16}
γGTP (U/l)	0.05	0.60	AFP (ng/ml)	0.42	8.1×10^{-6}
Female patients					
Albumin (g/dl)	−0.48	1.0×10^{-3}	Platelet count ($\times 10^9$/l)	−0.19	0.23
Total bilirubin (mg/dl)	0.18	0.25	Liver stiffness values (kPa)	0.40	0.025
AST (U/l)	0.28	0.067	APRI	0.25	0.22
ALT (U/l)	0.22	0.16	Hyaluronic acid (mg/L)	0.34	0.058
ALP (U/l)	0.21	0.17	Type IV collagen 7S (ng/ml)	0.42	0.016
γGTP (U/l)	0.45	3.0×10^{-3}	AFP (ng/ml)	0.37	0.016

Serum levels of type IV collagen 7S and hyaluronic acid were measured in 69 male and 32 female patients.

in peri-tumorous tissues were significantly correlated with liver fibrosis stage ($P = 6.3 \times 10^{-3}$, Jonckheere–Terpstra test), as demonstrated in Fig. 3E. There was also a significant correlation between ATX mRNA expression levels in peri-tumorous tissues and platelet counts as shown in Fig. 3F (Spearman's rank correlation coefficient; $\rho = -0.55$, $P = 1.6 \times 10^{-3}$).

4. Discussion

In the current study, increased serum ATX levels were observed in 89.5% of male RFA patients and all of female RFA patients with HCC, as expected. To explain this increase in serum ATX levels in HCC patients, there could have been 2 possibilities; one was that abundant production of ATX in HCC tissues might lead to increased serum ATX levels. Another possibility was that fibrosis in the background liver bearing HCC might cause the increase in serum ATX levels, because serum ATX activity was known to be increased correlatively with the liver fibrosis stage in chronic hepatitis C patients [30]. Of note, both possibilities were not mutually exclusive.

Table 3
Characteristics of patients who underwent hepatic resection.

Variable	$n = 30$
Age (y)	69.0 (63.0–74.5)
Sex, *n* (%)	
Male	22 (73.3)
Female	8 (26.7)
Viral markers, *n* (%)	
HBsAg, positive	5 (16.7)
Anti-HCVAb, positive	13 (43.3)
Both negative	12 (40.0)
AST (U/l)	36.0 (25.5–48.3)
ALT (U/l)	30.0 (21.3–48.5)
Albumin (g/dl)	3.9 (3.6–4.2)
Platelet count ($\times 10^9$/l)	152 (113–182)
Child Pugh classification	
Class A	28 (93.3)
Class B	2 (6.7)
Size of main tumor (cm)	2.2 (1.5–4.5)
No. of tumors[a]	
1	18 (60.0)
2	6 (20.0)
3	4 (13.3)
4	1 (3.3)
Serum ATX level (mg/l)[b]	1.20 ± 0.60
AFP (ng/ml)	10.2 (3.6–30.8)

Values are expressed as median and range (25th–75th percentiles), mean ± SD, or number (percent).
[a] The number of tumors was not counted in one patient with portal invasion.
[b] Serum ATX levels were measured in 26 patients.

To examine the first one, serum ATX levels were measured before and after RFA with curative intent. As a result, serum ATX levels were not decreased after RFA compared to those before, whereas serum AFP levels were significantly reduced after RFA. Furthermore, serum ATX levels were not associated with HCC burden. These results suggest that increased serum ATX levels in HCC patients may not be caused by elevated ATX production in HCC tissues. Evidence that serum ATX levels in HCC patients were not higher than those in C-CLD patients without HCC and were rather lower than those in cirrhotic patients may be in agreement with this speculation.

On the other hand, the strong correlations were observed between serum ATX levels and the parameters predicting for liver fibrosis, i.e., liver stiffness values, serum hyaluronic acid levels, serum type IV collagen 7S levels, and APRI. As described earlier, we previously reported that serum ATX activity was increased correlatively with the fibrosis stage in liver in humans [14] and rats [15], and that serum ATX levels were a useful marker for liver fibrosis in chronic hepatitis C patients [14,30]. As well known, HCC frequently develops in patients with advanced liver fibrosis [16–19]. Thus, these results raise a possibility that the increased serum ATX levels in HCC patients, who underwent RFA, may be rather explained by fibrosis in the background liver bearing HCC.

To examine whether ATX expression might be high in HCC tissues, as previously reported, we had a chance to directly analyze HCC tissues in surgically-treated patients. In contrast to the previous evidence, ATX mRNA expression in HCC tissues was not elevated, but rather lower compared to the background liver tissues in the current study. Nonetheless, there was no correlation between ATX mRNA expression in HCC tissues and serum ATX levels. Thus, we have concluded that serum ATX levels may not be associated with the status of HCC, but may rather reflect fibrosis in the background liver in HCC patients.

We could not find the higher ATX mRNA expression in HCC tissues compared to non-tumorous tissues in HCC patients treated with hepatic resection. In this regard, Cooper et al. previously reported that ATX mRNA was overexpressed in liver tissues of patients with HCC [17]. Because they analyzed ATX mRNA in HCC tissues compared with normal liver tissues, our current results may not be inconsistent with their results. However, Wu et al. further reported that the increased ATX antigen expression was detected mainly in HCC tissues compared to normal liver tissues and that ATX overexpression in HCC was specifically correlated with inflammation and liver cirrhosis [19]. According to their results, ATX was detected predominantly in HCC cells, which may be in contrast with our current findings, although the correlation with liver cirrhosis is in line with our findings. Furthermore, microarray data suggest that ATX mRNA was more strongly expressed in tumorous compared with paired non-tumorous tissues [18]. We cannot explain these differences between the previous studies and ours for the present. Our

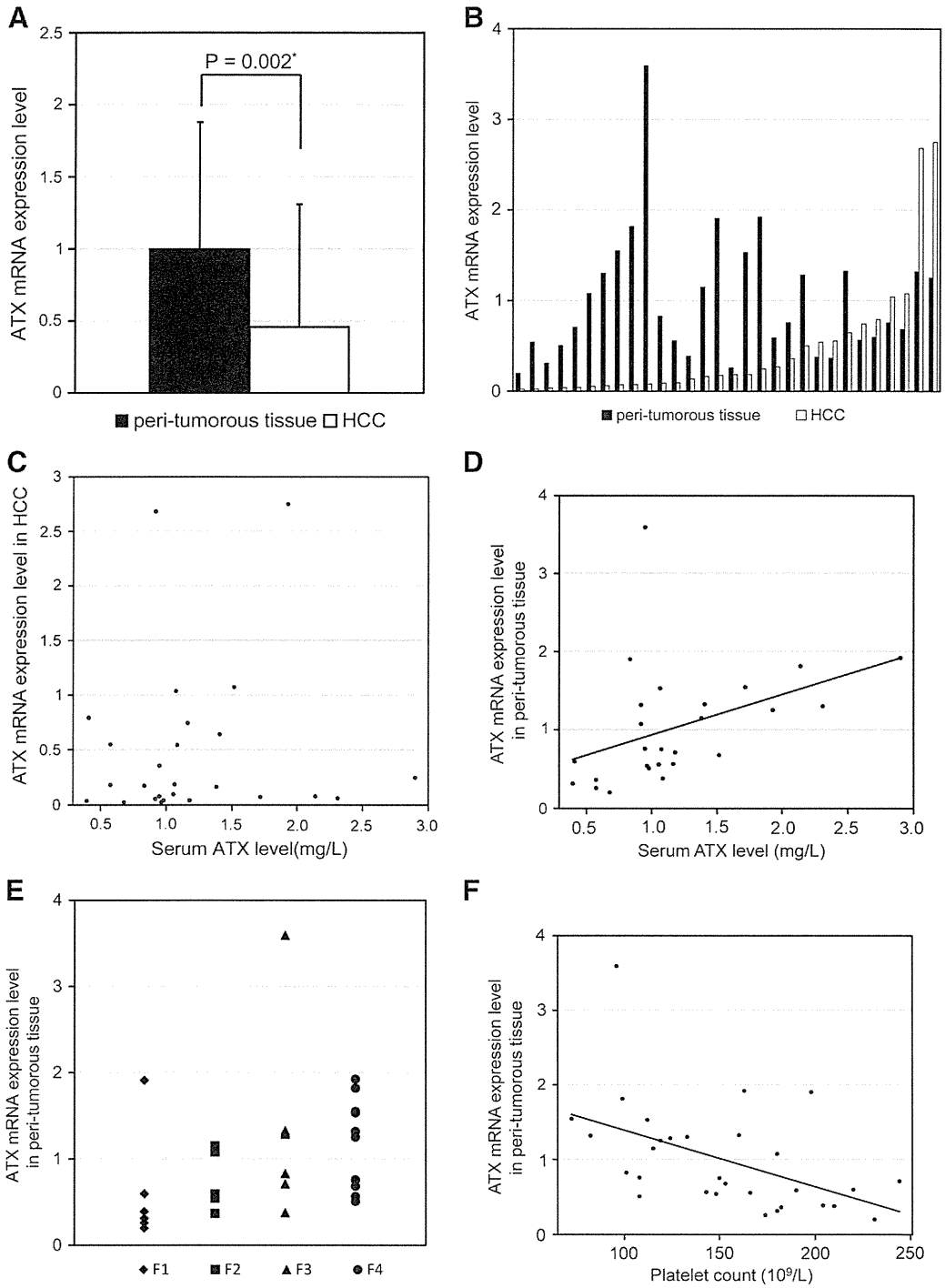

Fig. 3. ATX mRNA expression in HCC and peri-tumorous tissues in surgically-treated patients. Data from 30 HCC patients treated with hepatic resection were used to analyze ATX mRNA expression. ATX mRNA expression levels were even lower in HCC tissues than in peri-tumorous tissues (A). Columns are shown as mean ± SD in 30 patients. The differences between ATX mRNA expression levels in HCC tissues and in peri-tumorous tissues were analyzed by using Wilcoxon signed-rank test. The asterisk indicates the significant difference. ATX mRNA expression levels in HCC tissues than in peri-tumorous tissues are shown in each patient (B). Relationships between serum ATX levels and ATX mRNA expression levels in HCC (C) and peri-tumorous tissues (D) are shown. Data from 26 HCC patients treated with hepatic resection were used. Then, relationships between ATX mRNA expression levels in peri-tumorous tissues and liver fibrosis stage (E) or platelet counts (F) are shown. Data from 30 HCC patients treated with hepatic resection were used.

results are based on the data from a substantial number of patients, and we have analyzed ATX mRNA expression by quantitative real time PCR, suggesting that ATX mRNA expression in HCC tissues may be at least variable. No alteration of serum ATX levels after RFA for HCC and no correlation of serum ATX levels with HCC burden observed in the current study may be in agreement with the finding that ATX mRNA expression in HCC tissues was not abundant compared to that in non-tumorous tissues in HCC patients. This point should be further elucidated.

The origin and fate of serum ATX have not been fully elucidated yet. High ATX mRNA expressions were found in adipose tissue, brain, lung, duodenum and adrenals, and ATX mRNA expressions were determined at a substantial level in liver, skeletal muscle, heart, suggesting that ATX transcript is expressed in many tissues or organs [31]. On the other hand, ATX has been shown to be cleared from the circulation, taken up and degraded in liver sinusoidal endothelial cells [32]. During the process of liver fibrosis, liver sinusoidal endothelial cells are known to

undergo phenotypic changes with a loss of various receptors and liver sinusoidal endothelial fenestrae causing the capillarization of the sinusoids, thereby impairing the uptake of various substances by these cells [33]. Thus, it is speculated that the phenotypic changes in liver sinusoidal endothelial cells during liver fibrosis may lead to a reduction in ATX clearance by these cells, increasing the circulating ATX levels. In addition to this, it has been clarified in the current study that the mechanism underlying the increased serum ATX levels in liver fibrosis may involve the increased production of ATX in fibrotic liver. We previously showed that ATX mRNA expression was not altered in carbon tetrachloride-induced fibrotic livers compared to normal livers in rats [15]. Regarding this difference in the increase in ATX mRNA expression in fibrotic livers in rats and humans, ATX production in fibrotic livers may vary depending on etiology or species. To solve this question, the origin and fate of ATX in blood should be further clarified.

In the current study, we showed that serum ATX levels did not reflect the status of HCC, suggesting that ATX may not be a useful marker in blood for HCC. However, because it is now well known that ATX is responsible for the bulk of LPA production in blood [13], our current data suggest that HCC tissues are likely to be exposed to an abundance of LPA. In this context, the stimulatory effects of LPA on the growth and motility of HCC-derived cells in vitro were reported [34–36]. Thus, elevated ATX levels in blood, caused by liver fibrosis, may play a role in pathophysiology of HCC via LPA. This matter should be further elucidated.

References

[1] Stracke ML, Krutzsch HC, Unsworth EJ, et al. Identification, purification, and partial sequence analysis of autotaxin, a novel motility-stimulating protein. J Biol Chem 1992;267:2524–9.
[2] Stracke ML, Clair T, Liotta LA. Autotaxin, tumor motility-stimulating exophosphodiesterase. Adv Enzym Regul 1997;37:135–44.
[3] Baumforth KR, Flavell JR, Reynolds GM, et al. Induction of autotaxin by the Epstein–Barr virus promotes the growth and survival of Hodgkin lymphoma cells. Blood 2005;106:2138–46 [Epub 2005 Jun 2132].
[4] Kishi Y, Okudaira S, Tanaka M, et al. Autotaxin is overexpressed in glioblastoma multiforme and contributes to cell motility of glioblastoma by converting lysophosphatidylcholine to lysophosphatidic acid. J Biol Chem 2006;281:17492–500.
[5] Yang Y, Mou L, Liu N, Tsao MS. Autotaxin expression in non-small-cell lung cancer. Am J Respir Cell Mol Biol 1999;21:216–22.
[6] Stassar MJ, Devitt G, Brosius M, et al. Identification of human renal cell carcinoma associated genes by suppression subtractive hybridization. Br J Cancer 2001;85:1372–82.
[7] Debies MT, Welch DR. Genetic basis of human breast cancer metastasis. J Mammary Gland Biol Neoplasia 2001;6:441–51.
[8] Kehlen A, Englert N, Seifert A, et al. Expression, regulation and function of autotaxin in thyroid carcinomas. Int J Cancer 2004;109:833–8.
[9] Tokumura A, Majima E, Kariya Y, et al. Identification of human plasma lysophospholipase D, a lysophosphatidic acid-producing enzyme, as autotaxin, a multifunctional phosphodiesterase. J Biol Chem 2002;277:39436–42.
[10] Umezu-Goto M, Kishi Y, Taira A, et al. Autotaxin has lysophospholipase D activity leading to tumor cell growth and motility by lysophosphatidic acid production. J Cell Biol 2002;158:227–33.
[11] Moolenaar WH, van Meeteren LA, Giepmans BN. The ins and outs of lysophosphatidic acid signaling. Bioessays 2004;26:870–81.
[12] Aoki J, Taira A, Takanezawa Y, et al. Serum lysophosphatidic acid is produced through diverse phospholipase pathways. J Biol Chem 2002;277:48737–44 [Epub 42002 Sep 48726].
[13] Tanaka M, Okudaira S, Kishi Y, et al. Autotaxin stabilizes blood vessels and is required for embryonic vasculature by producing lysophosphatidic acid. J Biol Chem 2006;281:25822–30.
[14] Watanabe N, Ikeda H, Nakamura K, et al. Both plasma lysophosphatidic acid and serum autotaxin levels are increased in chronic hepatitis C. J Clin Gastroenterol 2007;41:616–23.
[15] Watanabe N, Ikeda H, Nakamura K, et al. Plasma lysophosphatidic acid level and serum autotaxin activity are increased in liver injury in rats in relation to its severity. Life Sci 2007;81:1009–15.
[16] Zhang G, Zhao Z, Xu S, Ni L, Wang X. Expression of autotaxin mRNA in human hepatocellular carcinoma. Chin Med J 1999;112:330–2.
[17] Cooper AB, Wu J, Lu D, Maluccio MA. Is autotaxin (ENPP2) the link between hepatitis C and hepatocellular cancer? J Gastrointest Surg 2007;11:1628–34 [discussion 1634–1625].
[18] Mazzocca A, Dituri F, Lupo L, Quaranta M, Antonaci S, Giannelli G. Tumor-secreted lysophostatidic acid accelerates hepatocellular carcinoma progression by promoting differentiation of peritumoral fibroblasts in myofibroblasts. Hepatology 2011;54:920–30.
[19] Wu JM, Xu Y, Skill NJ, et al. Autotaxin expression and its connection with the TNF-alpha-NF-kappaB axis in human hepatocellular carcinoma. Mol Cancer 2010;9:71.
[20] Ikeda H, Enooku K, Ohkawa R, Koike K, Yatomi Y. Plasma lysophosphatidic acid levels and hepatocellular carcinoma. Hepatology 2013;57:417–8.
[21] Torzilli G, Minagawa M, Takayama T, et al. Accurate preoperative evaluation of liver mass lesions without fine-needle biopsy. Hepatology 1999;30:889–93.
[22] Tateishi R, Shiina S, Teratani T, et al. Percutaneous radiofrequency ablation for hepatocellular carcinoma. An analysis of 1000 cases. Cancer 2005;103:1201–9.
[23] Teratani T, Yoshida H, Shiina S, et al. Radiofrequency ablation for hepatocellular carcinoma in so-called high-risk locations. Hepatology 2006;43:1101–8.
[24] Nakamura K, Igarashi K, Ide K, et al. Validation of an autotaxin enzyme immunoassay in human serum samples and its application to hypoalbuminemia differentiation. Clin Chim Acta 2008;388:51–8.
[25] Castera L, Vergniol J, Foucher J, et al. Prospective comparison of transient elastography, Fibrotest, APRI, and liver biopsy for the assessment of fibrosis in chronic hepatitis C. Gastroenterology 2005;128:343–50.
[26] Lebray P, Varnous S, Charlotte F, Varaut A, Poynard T, Ratziu V. Liver stiffness is an unreliable marker of liver fibrosis in patients with cardiac insufficiency. Hepatology 2008;48:2089.
[27] Sagir A, Erhardt A, Schmitt M, Haussinger D. Transient elastography is unreliable for detection of cirrhosis in patients with acute liver damage. Hepatology 2008;47:592–5.
[28] El-Serag HB, Rudolph KL. Hepatocellular carcinoma: epidemiology and molecular carcinogenesis. Gastroenterology 2007;132:2557–76.
[29] Nakamura K, Ohkawa R, Okubo S, et al. Measurement of lysophospholipase D/autotaxin activity in human serum samples. Clin Biochem 2007;40:274–7.
[30] Nakagawa H, Ikeda H, Nakamura K, et al. Autotaxin as a novel serum marker of liver fibrosis. Clin Chim Acta 2011;412:1201–6.
[31] Stefan C, Gijsbers R, Stalmans W, Bollen M. Differential regulation of the expression of nucleotide pyrophosphatases/phosphodiesterases in rat liver. Biochim Biophys Acta 1999;1450:45–52.
[32] Jansen S, Andries M, Vekemans K, Vanbilloen H, Verbruggen A, Bollen M. Rapid clearance of the circulating metastatic factor autotaxin by the scavenger receptors of liver sinusoidal endothelial cells. Cancer Lett 2009;284:216–21.
[33] Muro H, Shirasawa H, Kosugi I, Nakamura S. Defect of Fc receptors and phenotypical changes in sinusoidal endothelial cells in human liver cirrhosis. Am J Pathol 1993;143:105–20.
[34] Genda T, Sakamoto M, Ichida T, et al. Cell motility mediated by rho and Rho-associated protein kinase plays a critical role in intrahepatic metastasis of human hepatocellular carcinoma. Hepatology 1999;30:1027–36.
[35] Ayaki M, Mukai M, Imamura F, et al. Cooperation of fibronectin with lysophosphatidic acid induces motility and transcellular migration of rat ascites hepatoma cells. Biochim Biophys Acta 2000;1495:40–50.
[36] Sokolov E, Eheim AL, Ahrens WA, et al. Lysophosphatidic acid receptor expression and function in human hepatocellular carcinoma. J Surg Res 2013;180:104–13.

International Immunology, Vol. 26, No. 7, pp. 397–406
doi:10.1093/intimm/dxu040
Advance Access publication 25 February 2014

Activation-induced cytidine deaminase is dispensable for virus-mediated liver and skin tumor development in mouse models

Tung Nguyen[1], Jianliang Xu[1], Shunsuke Chikuma[1], Hiroshi Hiai[2], Kazuo Kinoshita[3], Kyoji Moriya[4], Kazuhiko Koike[5], Gian Paolo Marcuzzi[6], Herbert Pfister[6], Tasuku Honjo[1] and **Maki Kobayashi[1]**

[1]Department of Immunology and Genomic Medicine, Graduate School of Medicine, Kyoto University, Kyoto 606-8501, Japan
[2]Medical Innovation Center, Graduate School of Medicine, Kyoto University, Kyoto 606-8501, Japan
[3]Shiga Medical Center Research Institute, Moriyama, Shiga 524-8524, Japan
[4]Department of Infection Control and Prevention, University of Tokyo, Bunkyo, Tokyo 113-8655, Japan
[5]Department of Gastroenterology, University of Tokyo, Bunkyo, Tokyo 113-8655, Japan
[6]Institute of Virology and Center for Molecular Medicine Cologne, University of Cologne, Cologne D-50931, Germany

Correspondence to: T. Honjo; E-mail: honjo@mfour.med.kyoto-u.ac.jp

Received 26 December 2013, *accepted* 10 February 2014

Abstract

Activation-induced cytidine deaminase (AID) not only promotes immune diversity by initiating somatic hypermutation and class switch recombination in immunoglobulin genes but also provokes genomic instability by introducing translocations and mutations into non-immunoglobulin genes. To test whether AID is essential for virus-induced tumor development, we used two transgenic tumor models: mice expressing hepatitis C virus (HCV) core proteins (HCV-Tg), driven by the hepatitis B virus promoter, and mice expressing human papillomavirus type 8 proteins (HPV8-Tg), driven by the Keratin 14 promoter. Both strains were analyzed in the absence and presence of AID by crossing each with *AID*$^{-/-}$ mice. There was no difference in the liver tumor frequency between the HCV-Tg/*AID*$^{+/+}$ and HCV-Tg/*AID*$^{-/-}$ mice at 20 months of age although the *AID*$^{+/+}$ mice showed more severe histological findings and increased cytokine expression. Furthermore, a low level of AID transcript was detected in the HCV-Tg/*AID*$^{+/+}$ liver tissue that was not derived from hepatocytes themselves but from intra-hepatic immune cells. Although AID may not be the direct cause of HCV-induced oncogenesis, AID expressed in B cells, not in hepatocytes, may prolong steatosis and cause increased lymphocyte infiltration into HCV core protein-induced liver lesions. Similarly, there was no difference in the time course of skin tumor development between the HPV8-Tg/*AID*$^{-/-}$ and HPV8-Tg/*AID*$^{+/+}$ groups. In conclusion, AID does not appear to be required for tumor development in the two virus-induced tumor mouse models tested although AID expressed in infiltrating B cells may promote inflammatory reactions in HCV core protein-induced liver pathogenesis.

Keywords: hepatitis C virus, human papillomavirus type 8

Introduction

Activation-induced cytidine deaminase (AID) is essential for inducing DNA breaks during the somatic hypermutation and class switch recombination of immunoglobulin genes required for generating antibody diversity in activated B cells (1). AID generates physiological mutations during deliberate antibody development, but can also cause chromosomal translocations and mutations in proto-oncogenes when expressed aberrantly (2). Transgenic, ubiquitous over-expression of AID causes T-cell lymphoma and micro-adenoma in the lung (3) along with mutations in the TCR and c-myc genes. Chronic infections with micro-organisms such as helicobacter pylori (4), hepatitis C virus (HCV) (5–7), and human T-cell leukemia virus type 1 (8) induce the aberrant AID expression, which has been proposed to cause tumors by introducing translocations and somatic mutations into proto-oncogenes. In addition, AID expression is associated with chronic infections of these pathogens in human cases, in which it has also been proposed to contribute to tumor formation at least in part (4, 9). However, it has not been directly determined if virus- or bacteria-induced oncogenesis requires the action of AID.

Hepatocellular carcinoma (HCC) is the fifth most frequent cancer, and hepatitis B virus (HBV) and HCV infections are

the major risk factors for developing this cancer worldwide (10). In fact the risk of developing HCC is increased 11.5- to 17-fold in HCV-infected patients; however, antiviral therapies have limited effectiveness in only a small fraction of patients. Thus, elucidation of the mechanism(s) involved in promoting liver tumorigenesis is urgently required for developing a prevention strategy. As natural infection of HCV is restricted to humans and chimpanzees, several transgenic mouse models harboring parts of the HCV polyprotein have been generated to recapitulate HCC development (11). HCV, a small RNA virus, belongs to the Flaviviridae family and contains a 9.6-kb single-stranded RNA genome. The polyprotein encoded by the HCV genome is processed into the structural proteins (including core, E1 and E2) and the non-structural (NS) proteins (NS2-NS5) required for RNA genome replication by host and viral proteases (11). Among them, the HCV core protein has unique, multifunctional roles in apoptosis, signal transduction, reactive oxygen species formation, transformation and immune modulation (such as the up-regulation of TGF-β) (10) by interacting with many cellular proteins. Out of the 14 lines of HCV-transgenic mice developed, 5 HCV core protein-containing transgenic lines and 1 non-structural (NS5A) transgenic line can give rise to HCC, after the development of severe steatosis, a characteristic pathology associated with HCV infection (11–13). Especially, a transgenic mouse model expressing HCV core protein (HCV-Tg) driven HBV regulatory elements (12), which limits HCV core protein expression strictly in hepatocytes, had the highest HCC prevalence among many HCV protein transgenic model mice (11, 13); therefore, this model mouse line seemed to be a good tool to investigate AID expression in hepatocytes and its contribution to the mechanism of HCC development.

On the other hand, the human papillomavirus (HPV) family of small DNA tumor viruses, of which there are over 120 types, can cause hyper-proliferative lesions in cutaneous and mucosal epithelia (14). Among them, HPV5 and HPV8 are classified as high-risk beta-type papilloma viruses and are the two major causes of cutaneous squamous cell carcinoma (SCC) in epidermodysplasia verruciformis patients. The development of SCC by HPV8 is promoted by a series of carcinogenic events, including DNA damage, evasion of apoptosis, mutation mediated by E6 protein and enhanced proliferation after ultraviolet light B exposure, mediated by E7 protein (14). Unlike HCV infection, HPV8 does not cause severe inflammation; however, DNA damage is an important carcinogenic process associated with this virus. A transgenic mouse model in which HPV8 early genes are expressed under the control of the Keratin 14 (K14) promoter (15) exhibits significant papilloma development (up to 91% of the HPV8-Tg mice) and malignant progression (6% of the HPV8-Tg mice backcrossed to FVB/N).

To determine whether AID is aberrantly induced by HCV or HPV8 and required for virally induced tumorigenesis, we crossed HCV-Tg or HPV8-Tg mice with *AID*$^{-/-}$ mice and compared the tumorigenesis frequencies in the *AID*$^{+/+}$ and *AID*$^{-/-}$ mice. We also examined the AID expression levels in the affected tissues. We found that HCV-Tg mice exhibited enhanced AID expression in the B cells infiltrating the liver, and that the steatosis and lymphocytic follicle formation were more severe in the HCV-Tg/*AID*$^{+/+}$ than in the HCV-Tg/*AID*$^{-/-}$ mice. However, the HCC prevalence at 20 months of age was not remarkably different between the two groups. Similarly, the time course of papilloma development was indistinguishable between the HPV8-Tg/*AID*$^{+/+}$ and HPV8-Tg/*AID*$^{-/-}$ mice. Furthermore, AID expression was not induced in the skin papillomatous tissues of the HPV8-Tg/*AID*$^{+/+}$ mice. We conclude that AID is not necessary for the viral protein-induced oncogenesis in these two mouse models.

Methods

Mouse maintenance and genotyping

All the mice used in this study were maintained at the Institute of Laboratory Animals in accordance with the guidelines of the Animal Research Committee, Graduate School of Medicine, Kyoto University. *AID*$^{-/-}$ mice (16) backcrossed to C57/B6 (B6) were crossed with HCV core protein transgenic mouse line (HCV-Tg) (12, 13) and HPV8-Tg mice (on an FVB/N background) (15). AID-Cre and Rosa-RFP compound mice (17) were crossed with HCV-Tg mice to enable the detection of previous and current AID expression. The genotyping primers are described in Supplementary Table 1, available at *International Immunology* Online.

Western blotting

Western blotting was performed by conventional methods. Mouse organs were dissected and homogenized in RIPA buffer. The primary antibodies used were the rat monoclonal anti-mouse AID antibody 2 (MAID-2) (eBioscience, San Diego, CA, USA), anti-Tubulin antibody (Calbiochem, MERCK, Darmstadt, Germany) and anti-HCV core protein antibody (clone B2, Yes Biotech Lab, Anogen, Ontario, Canada).

Reverse transcription–PCR and quantitative reverse transcription–PCR

Mouse organs were excised and homogenized in Sepasol RNA I Super (Nacalai Tesque, Kyoto, Japan) following the manufacturer's instructions. Reverse transcription–PCR (RT–PCR) was performed as previously described (18). ExTaq DNA polymerase (TaKaRa, Shiga, Japan) and the primers described in Supplementary Table 2, available at *International Immunology* Online, were used for conventional PCR. Real-time PCR was performed with the primer sets in Supplementary Table 2, available at *International Immunology* Online, and the Power SYBR Green PCR Master Mix (ABI, Life Technologies Japan, Tokyo, Japan) using the ABI 7900HT system (ABI). The delta-delta Ct method was used to calculate the fold change in gene expression. Error bars show the standard deviation.

Histology and immunohistochemistry

For AID immunohistochemical staining, freshly excised livers were fixed in 4% paraformaldehyde and processed for frozen section as previously described (19). AID protein was detected by MAID-2 and peroxidase-labeled donkey F(ab′)2 anti-rat IgG (Jackson ImmunoResearch, West Grove, PA, USA) and stained with diaminobenzidine. Images were

captured with a DM5000B microscope (Leica; Wetzlar, Germany). Hematoxylin and eosin (H&E)-stained samples were fixed with Mildform 10N (Wako Pure Chemical Industries, Osaka, Japan), embedded in paraffin and stained by standard methods.

Liver cell fractionation and FACS analysis

The isolation of intra-hepatic immune cells (IHICs) from the liver of HCV-Tg mice was performed as previously described, with some minor modifications (20). The composition of IHIC cells was assessed by staining with the following antibodies: PE-labeled anti-mouse B220 for B cells, allophycocyanin (APC)-conjugated anti-mouse CD11b for macrophages and FITC-labeled anti-mouse CD8 and APC-anti-mouse CD4 for T cells. The stained cells were analyzed on a FACSCalibur (BD Japan, Tokyo).

ELISA

TNF-α, IL-1β and TGF-β were detected using ELISA kits specific for each cytokine (BioSource, Life Technologies), according to the manufacturer's instructions.

Statistical analysis

The Mann–Whitney *U*-test was used to calculate the statistical differences in AID expression (Fig. 1B). Fisher's exact test was used to determine significant differences in tumor incidence (Table 3). Student's *t*-test was used to determine significant differences in cytokine expression (Fig. 3B and C), and Welch's *t*-test was used for pathological severity validation (Table 2). *P* values < 0.05 were considered statistically significant.

Results

Increased AID transcripts in the liver of HCV-Tg mice

To generate the observation groups, HCV-Tg mice were crossed with *AID*$^{-/-}$ mice. Then HCV-Tg/AID$^{+/-}$(HCV(+)AID$^{+/-}$) mice from the first filial generation were again crossed each other and the obtained HCV(+)AID$^{-/-}$ and HCV(+)AID$^{+/+}$ mice of the second filial generation were compared as the observation groups. The expression level of the HCV core protein in the liver was similar in the HCV(+)AID$^{-/-}$ and HCV(+)AID$^{+/+}$ mice (Supplementary Figure 1, available at *International Immunology* Online). Because HCV-Tg mice develop severe steato-hepatitis within 9 months after birth (12), and this chronic inflammation is supposed to reproduce the similar cytokine environment to the TNF-α-stimulated hepatocyte cell lines that express AID (9), we examined AID expression in the liver. AID transcripts were detected in the liver from 16-month-old HCV(+)AID$^{+/+}$ mice, but not from wild-type B6 mice (Fig. 1A, Supplementary Figure 2, available at *International Immunology* Online). However, the AID expression detected in the HCV(+)AID$^{+/+}$ liver was comparable to the low levels observed in primary unstimulated spleen cells, which included B and T lymphocytes. Transcripts for CD19, a specific marker for B lymphocytes, were also higher in the HCV(+) compared with the B6 liver, suggesting that the HCV(+) liver may contain a considerable number of B

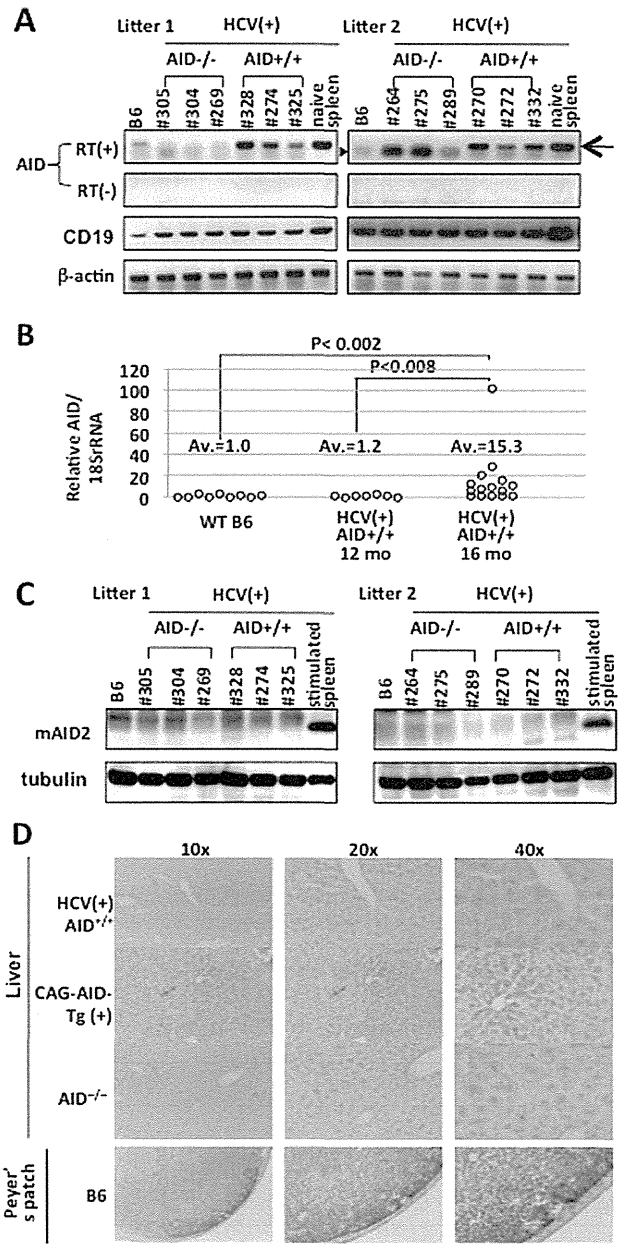

Fig. 1. AID expression in the liver of HCV-Tg mice. (A) Representative RT–PCR analysis showing AID mRNA expression in the liver of 16-month-old HCV(+)AID$^{+/+}$ mice. Naive spleen RNA was included as a positive control. Numbers indicate individual mice. RT(+), with reverse transcriptase; RT(−), without reverse transcriptase. The arrow indicates primer-specific amplification, and the arrowhead shows non-specific amplification. (B) Relative AID expression level in the liver of HCV(+)AID$^{+/+}$ mice at 16 months (n = 15) and 12 months of age (n = 7) and in wild-type (WT) 16-month-old (B6) mice (n = 9), determined by quantitative (q) RT–PCR. *P* value by Mann–Whitney *U*-test. (C) AID protein in the liver of the 16-month-old HCV-Tg mice analyzed in (A), determined by western blot. Splenocytes stimulated with IL-4 and LPS for 3 days were used as a positive control. (D) Immunohistochemistry for AID protein localization in the liver of HCV-Tg mice. The Peyer's patches and liver of a CAG-AID-Tg (CAG promoter-driven AID Tg) mouse were included as positive controls, and the liver of an AID$^{-/-}$ mouse was included as a negative control.

Table 1. AID, CD19 and albumin mRNA levels in purified IHICs and hepatocytes

	CD19/18s rRNA			Albumin/18s rRNA		AID/18s rRNA		
	IHICs	Hepatocytes	Spleen B cells	IHICs	Hepatocytes	IHICs	Hepatocytes	Spleen B cells
B6	326.6	3.3	920.0	1.0	1171.3	7.0±0.30	1.0	338.6±11.7
HCV(+)AID$^{-/-}$	306.1	1.3		0.27	1082.0	0.0	0.0	
HCV(+)AID$^{+/+}$	360.6	1.0		10.6	1027.2	132.6±11.0	3.2±0.63	

Relative AID/18s rRNA expression in B6 hepatocyte is set as 1.0, relative CD19/18s rRNA in HCV(+)AID$^{+/+}$ as 1.0 and relative Albumin/18s rRNA in B6 as 1.0. Zero means undetectable signal by q-PCR.

Table 2. The scored histological phenotypes of HCV(+)AID$^{-/-}$ and HCV(+)AID$^{+/+}$ mice

	Genotype of AID	Severity score				
		0	1	2	3	Average
Steatosis in HCV(+)						
12 months	−/−	0	0	0	3	3
	+/+	0	0	0	2	3
16 months	−/−	2	8	2	0	1.00*
	+/+	0	8	4	0	1.33
20 months	−/−	9	7	1	4	1.00*
	+/+	3	12	2	4	1.33
Lymphoid follicle in HCV(+)						
16 months	−/−	9	3	0	0	0.25*
	+/+	5	7	0	0	0.58
20 months	−/−	4	13	1	3	1.14*
	+/+	2	11	4	4	1.48

The severity of steatosis and lymphoid follicle formation is classified as: 0 (none), 1 (mild), 2 (moderate) or 3 (severe). Values are the numbers of mice with each score.
*AID$^{-/-}$ versus AID$^{+/+}$, $P > 0.05$ by Welch's *t*-test.

Table 3. Liver tumor incidence in HCV-Tg mice

Age	16 months		20 months	
AID genotype	−/−	+/+	−/−	+/+
Male/Female	0/15	0/15	21/0	21/0
Tumour	0	0	3	4
Malignancy	0	0	2	4*

*AID$^{-/-}$ versus AID$^{+/+}$, $P > 0.05$ by Fisher's exact test.

lymphocytes, which could contribute to the increased AID expression. Real-time PCR analysis revealed that the AID transcript level in the liver from 16-month-old HCV(+)AID$^{+/+}$ females was 15-fold greater than that from the liver of similarly aged B6 mice and of 12-month-old HCV(+)AID$^{+/+}$ males (Fig. 1B).

The AID protein levels were measured in the same liver samples by western blotting (Fig. 1C). However, using MAID-2, no protein signal could be detected in the same samples that contained AID transcripts (Fig. 1A). To quantify the limitation of AID protein detection by MAID-2, we used spleen cells as a control (Supplementary Figure 3, available at *International Immunology* Online). We assigned one arbitrary unit of AID mRNA to the q-PCR signal detected from 500 ng of naive spleen cell RNA. Extracts prepared from the same number of spleen cells contained 8.6 μg protein, which did not elicit a detectable AID signal in the western blot. Since the AID transcript level from the HCV(+)AID$^{+/+}$ samples in Supplementary Figure 2, available at *International Immunology* Online, was lower than that in naive spleen cells, we conclude that the AID protein signal in the HCV(+)AID$^{+/+}$ liver was below the level detected by MAID2.

We next explored the possibility that the AID protein expression was limited to a specific location in the liver, such as the immune cells in the hepatic blood vessels. We therefore performed an immunohistochemical analysis of AID (Fig. 1D). Although positive controls including liver tissue from CAG-promoter-driven AID transgenic mice (3) and Peyer's patches from B6 wild-type mice showed clear brownish signals, there was no signal detected in any part of the HCV(+)AID$^{+/+}$ liver tissue samples.

AID transcripts are detected in IHICs, but not in hepatocytes from HCV-Tg mice

We next explored the possibility that the low level of AID transcripts was contributed by B cells infiltrating the HCV-Tg liver. Liver cells from three HCV(+)AID$^{-/-}$ or HCV(+)AID$^{+/+}$ mice at 16 months of age were fractionated to separate the IHICs from the hepatocytes (Fig. 2A and B). RNA was purified from both fractions of each genotype, and the AID, CD19 and albumin transcripts were analyzed to confirm the purity of these fractions and to identify the cellular origin of the AID mRNA (Table 1). CD19 transcripts were detected almost exclusively in IHICs, while albumin transcripts were mostly in hepatocytes, validating the fractionation procedure. The level of AID transcripts detected in the HCV(+)AID$^{+/+}$ IHICs was comparable to the level observed in splenic B cells (132.6±11.0 versus 338.6±11.7, respectively), while the level in hepatocytes was much lower, indicating that the source of AID transcripts in the liver was not the hepatocytes themselves but the IHICs. Cell surface marker analysis by FACS revealed that the IHICs consisted of B220$^+$ B cells (25–29%), CD4$^+$ or CD8$^+$ T cells (~45%) and CD11b$^+$ cells (7–10%), and that this composition was not notably changed by the presence of the HCV transgene or the AID genotype at 16 months of age (Fig. 2A, Supplementary Table 3, available at *International Immunology* Online).

To detect both current and past AID expression, transgenic reporter mice expressing tdRFP under the control of BAC-AID-Cre (17) were crossed to HCV-Tg mice (Fig. 2B and C, Supplementary Table 3, available at *International Immunology* Online). This mouse line reveals tdRFP fluorescence in any cells that have (or had) expressed AID. Using this approach, tdRFP$^+$ cells were found to represent

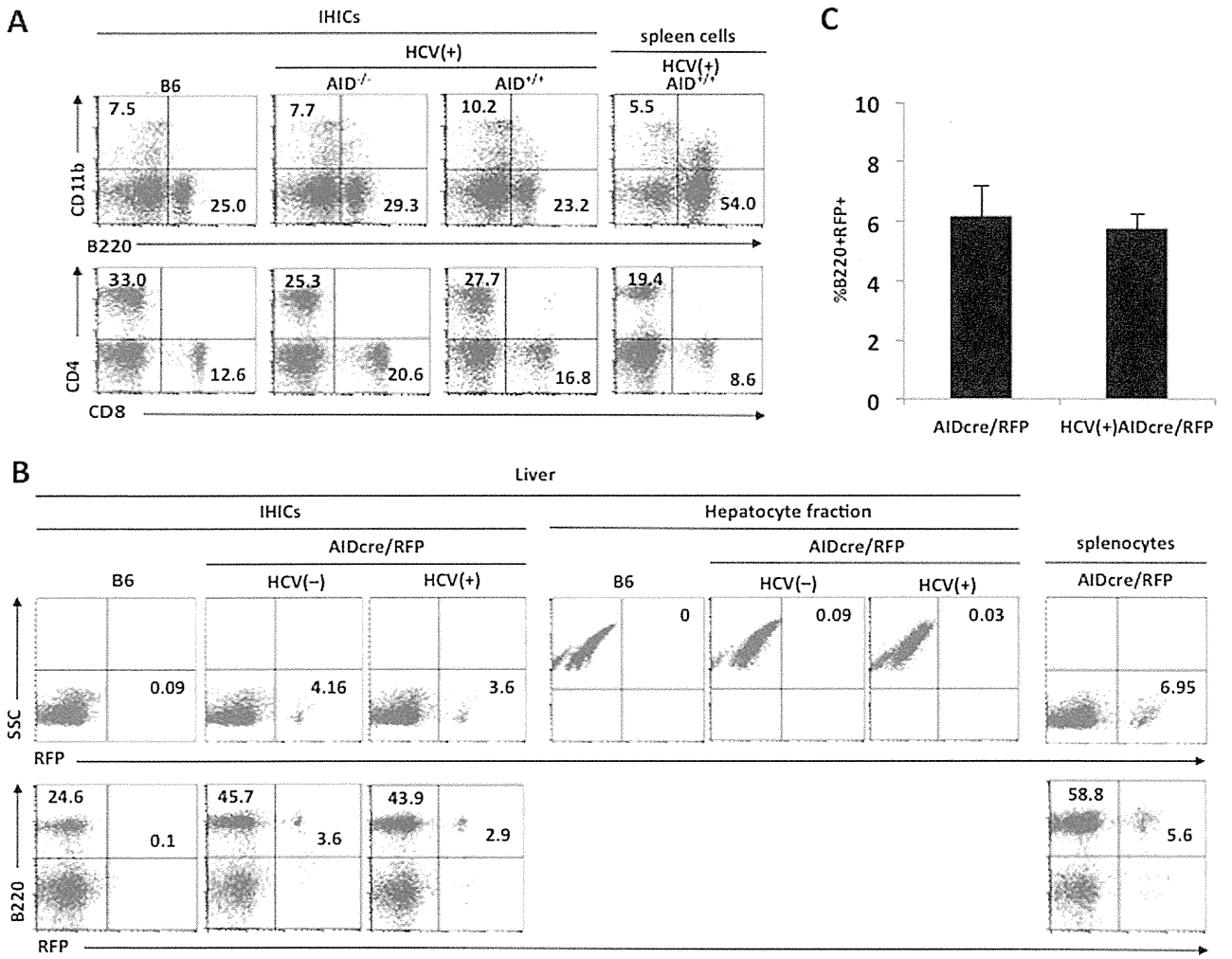

Fig. 2. Cell surface marker analysis of IHICs and hepatocytes from HCV-Tg mice. (A) Cell surface marker profile of IHICs revealed by FACS analysis. The numbers indicate the percentage of each population. The data are representative of three independent experiments. (B) AID expression represented by the tdRFP reporter in the IHICs and hepatocytes from the liver of 3-month-old HCV(+)AIDcre/RFP and HCV(−) AIDcre/RFP mice. The FACS profile data shown in (B and C) are representative of three independent experiments. The definitive cell numbers of each quadrant in (B and C) are shown in Supplementary Table 3, available at *International Immunology* Online. (C) Average percentage of $B220^+RFP^+$ cells in the $B220^+$ IHIC population from three independent experiments.

3–4% of the total IHICs in both HCV-Tg and no HCV-Tg (HCV(−)) mice at 3 months of age (Fig. 2B). tdRFP was not detected in hepatocytes from 3-month-old HCV(+) mice that had already developed mild steato-hepatitis (12). Analysis of three mice of each genotype (HCV(+) and HCV(−)) revealed that the $tdRFP^+$ cells represented $5.8 \pm 0.45\%$ versus $6.2 \pm 1.0\%$ of the $B220^+$ population, respectively (Fig. 2C), indicating that the presence of the HCV transgene did not affect the AID gene expression in mice during the first 3 months of life.

AID deficiency reduces the severity of histopathological phenotypes and cytokine expression profiles in the liver of HCV-Tg mice

It is reported that 14–30% of HCV-Tg male mice develop HCC between 16 and 19 months of age (13). We therefore analyzed the histopathological phenotypes of H&E-stained liver sections from $HCV(+)AID^{-/-}$ and $HCV(+)AID^{+/+}$ mice at 12 (male), 16 (female) and 20 months (male) of age (Figs 3A and 4A and Table 2). The severities of steatosis and lymphocyte infiltration were graded from 0 to 3, and the average scores for each group were calculated and tested by Welch's *t*-test (Table 2).

At 12 months of age, both $HCV(+)AID^{-/-}$ and $HCV(+)AID^{+/+}$ male mice had developed severe steatosis. Unexpectedly, the steatosis was milder in both $HCV(+)AID^{-/-}$ and $HCV(+)AID^{+/+}$ female mice at 16 months of age than $HCV(+)AID^{-/-}$ and $HCV(+)AID^{+/+}$ male mice at 12 months of age. The steatosis in the $HCV(+)AID^{+/+}$ mice appeared to be more severe than in $HCV(+)AID^{-/-}$ mice, but the difference was not significant ($P > 0.05$). This decrease in steatosis severity may have been due to the female composition of the mice because females of this HCV-Tg line did not show tumor development

(13), and human HCV-infected cirrhotic females develop HCC less frequently (21). In addition, lymphoid follicle formation was apparent at 16 months of age and was more frequent in the HCV(+)AID$^{+/+}$ than the HCV(+)AID$^{-/-}$ mice (Fig. 3A; Table 2). Consistent with the previous report (13), the fibrotic or regenerative nodular changes were very mild at 16 months of age.

However, the liver samples from both HCV(+)AID$^{-/-}$ and HCV(+)AID$^{+/+}$ mice at 20 months of age revealed marked progressive changes, with nuclear atypia detected in 10 out of 21 of each genotype, and liver cell degeneration or regenerative changes detected in 10 and 11 out of 21 HCV(+)AID$^{-/-}$ and HCV(+)AID$^{+/+}$ mice, respectively (Fig. 4A). Interestingly, both the steatosis and lymphoid follicle severity scores appeared to be higher in the HCV(+)AID$^{+/+}$ than the HCV(+)AID$^{-/-}$ 20-month-old mice (1.33 versus 1.00 for steatosis and 1.48 versus 1.14 for lymphoid follicles, respectively) although the observed differences were not statistically significant (Table 2).

We next examined whether the more advanced inflammatory histological phenotypes observed in the HCV(+)AID$^{+/+}$ mice were associated with increases in cytokine expression. Since cytokine production levels are altered in chronic HCV hepatitis (22) and in HCV-Tg mouse (23), we used q-PCR to measure representative pro-inflammatory T_h1 and T_h2 cytokine expression levels in the livers of 16-month-old female mice (Fig. 3B). The presence of the HCV transgene was associated with significantly higher levels of IL-1β, TNF-α and TGF-β mRNA, and HCV(+)AID$^{+/+}$ mice exhibited higher TNF-α levels than HCV(+)AID$^{-/-}$ mice. Consistent with the q-PCR results, the protein levels of IL-1β and TGF-β were also elevated by the presence of the HCV transgene, and the TNF-α protein production level was dependent on the presence of AID, suggesting that TNF-α production may have led to the aggressive pathological findings observed in HCV(+)AID$^{+/+}$ mice (Fig. 3C).

Similar tumor incidence in HCV(+)AID$^{-/-}$ and HCV(+) AID$^{+/+}$ mice

The incidence of tumor formation was carefully examined by histopathological and macroscopic evaluation. None of the 15 HCV(+)AID$^{-/-}$ or 15 HCV(+)AID$^{+/+}$ 16-month-old female mice showed evidence of liver tumor formation, consistent with a previous report (Table 3) (13). Further analysis of the 20-month-old male groups, including 21 HCV(+)AID$^{-/-}$ and 21 HCV(+) AID$^{+/+}$ mice, revealed that 4 out of 21 HCV(+)AID$^{+/+}$ mice carried macroscopic tumors, all of which were determined to be malignant by histological examination (Fig. 4A, right 4 panels). Similarly, 3 out of 21 HCV(+)AID$^{-/-}$ mice bore macroscopic tumors, two of which were judged to be malignant (Fig. 4A, left 3 panels). These results suggest that AID is not essential for HCV-induced carcinogenesis. Consistent with these findings, the AID transcript level in the tumor region of an AID$^{+/+}$ mouse (#241) was equivalent to the level detected in a non-tumor area (Fig. 4B). Comparison of the AID expression in the tumor and non-tumor areas from the two tumor-bearing mice of the HCV(+)AID$^{-/-}$ and the two of HCV(+)AID$^{+/+}$ indicated that the tumor tissues did not contain elevated AID expression levels (Fig. 4C). The AID protein levels were not detectable by western blotting in either the tumor or non-tumor areas (Fig. 4D).

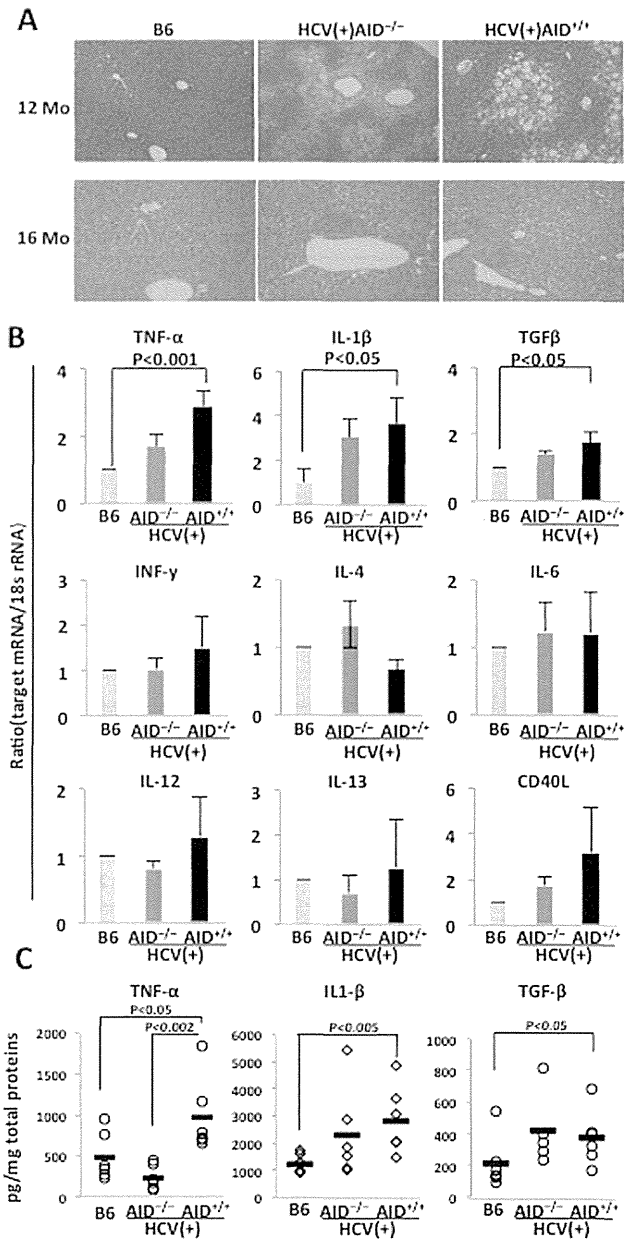

Fig. 3. Inflammatory responses in the liver of HCV(+)AID$^{-/-}$ and HCV(+)AID$^{+/+}$ mice. (A) Representative liver histology shown by H&E staining. Wild-type B6 mice (left panel), HCV(+)AID$^{-/-}$ (middle panel) and HCV(+)AID$^{+/+}$ (right panel) mice at 12 and 16 months of age (original magnification ×200). (B) mRNA expression of pro-inflammatory, T_h1 and T_h2 cytokines in the liver of 16-month-old mice. $n = 3$ (mean ± SD). (C) ELISA detection of cytokines in whole liver lysates from 16-month-old wild-type B6, HCV(+)AID$^{-/-}$ and HCV(+)AID$^{+/+}$ mice. The data shown for each of the groups are based on the values from six mice, except for the IL1-β evaluation for the HCV(+)AID$^{+/+}$ group, which is based on five mice.

Dispensability of AID for the development of skin tumors in HPV8-Tg mice

To examine AID's involvement in the development of HPV8-induced skin tumors, HPV8-Tg (HPV(+)) mice were crossed with AID$^{-/-}$ mice. Then HPV8(+)AID$^{+/-}$ mice of the first filial

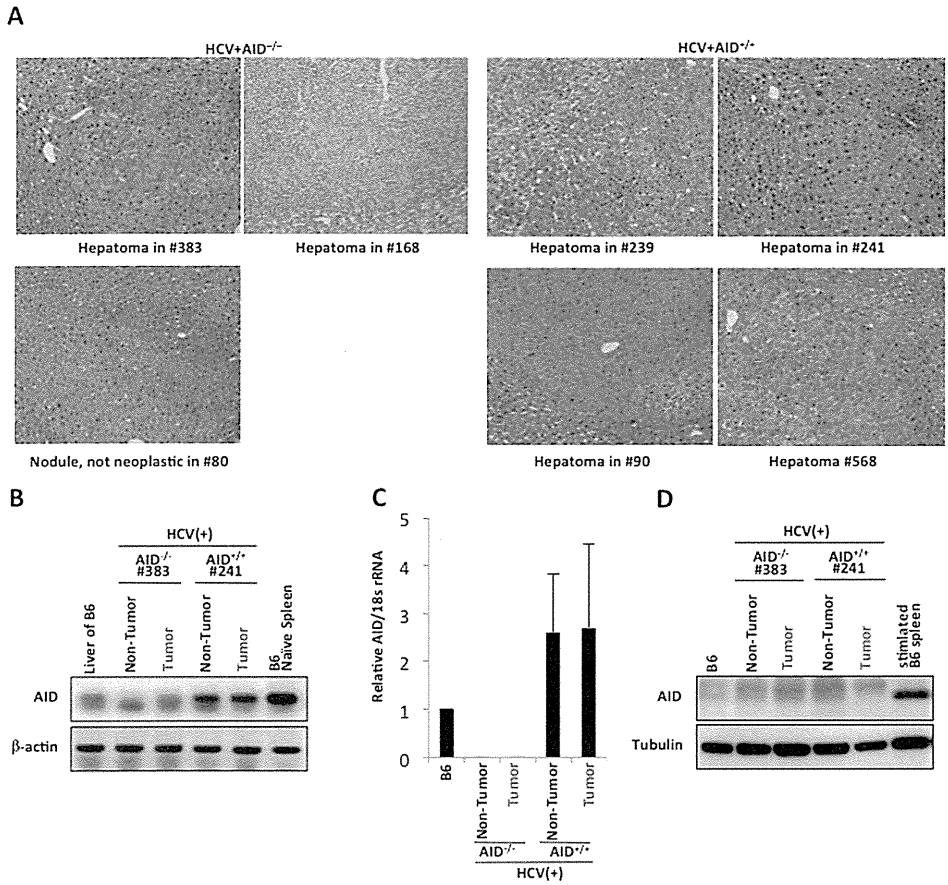

Fig. 4. Development of hepatocellular carcinoma in HCV-Tg mice. (A) H&E staining of the tumors found in HCV(+)AID$^{+/+}$ and HCV(+)AID$^{-/-}$ mice (original magnification ×200). (B) Representative AID mRNA expression profile in the tumor and non-tumor regions of HCV(+)AID$^{-/-}$ (#383) and HCV(+)AID$^{+/+}$ (#241) mice. (C) Quantitative RT–PCR of AID mRNAs analyzed as in (B). Error bars show standard deviation from two mice of each group. (D) Western blot analysis of AID protein in samples from the same mice analyzed in (B).

generation were again crossed each other and the obtained HPV8(+)AID$^{-/-}$ and HPV8(+)AID$^{+/+}$ mice of the second filial generation were compared as the observation groups. Both genotypes developed skin tumors, and tumor samples from 6-month-old mice were tested for AID expression by RNA and protein analyses (Fig. 5A and B). Neither the AID protein nor its RNA was detectable in the samples analyzed. After 6 months, the final skin tumor prevalence was ~30% in both mouse populations (15 out of 49 HPV8(+)AID$^{-/-}$ and 16 out of 51 HPV8(+)AID$^{+/+}$) (Supplementary Table 4, available at *International Immunology* Online), and the frequency and time course of tumor development in the two groups were almost indistinguishable (Fig. 5C). The histological examination of the skin tumor did not show any difference between HPV8(+)AID$^{+/+}$ and HPV8(+)AID$^{-/-}$ mice (Fig. 5D). The lower papilloma prevalence (~30%) compared to the original report describing the HPV8(+) mice (15) may be due to the mixed genetic background of FVB/N and B6 in both groups (the HPV8(+)AID$^{-/-}$ and HPV8(+)AID$^{+/+}$ mice), since mice with an FVB/N genetic background are reported to have more severe papilloma progression than those with a B6 background (15). Although the malignant progression to SCC in these skin tumors was not examined, AID expression was absent, and tumor development was equivalent in the AID$^{-/-}$ and AID$^{+/+}$ mice. We thus conclude that AID is not involved in HPV8-induced skin tumorigenesis.

Discussion

In this study, we investigated the requirement of AID for virally induced tumorigenesis by using compound mice that were generated by crossing mice transgenic for either HCV core proteins or HPV8 early proteins with either AID wild-type or knockout mice. Our results indicated that AID was expressed in neither hepatocytes of HCV-Tg nor skin tissue of HPV8-Tg. Thus, AID was not shown to be required for the development of both HCV- and HPV8-promoted tumorigenesis. We could not conclude that the frequency of the liver malignancy is statistically different between HCV(+)AID$^{+/+}$ (4 out of 21 mice) and HCV(+)AID$^{-/-}$ (2 out of 21 mice), partly because the frequency of the liver malignancy was unexpectedly lower than that in the original report (13). Studies on 5 times the number of mice may allow us to obtain statistically significant conclusions about the frequency of the liver malignancy between HCV(+)AID$^{+/+}$ and HCV(+)AID$^{-/-}$ mice. We note, however, that the HCV(+)AID$^{+/+}$ mice exhibited higher levels of TNF-α

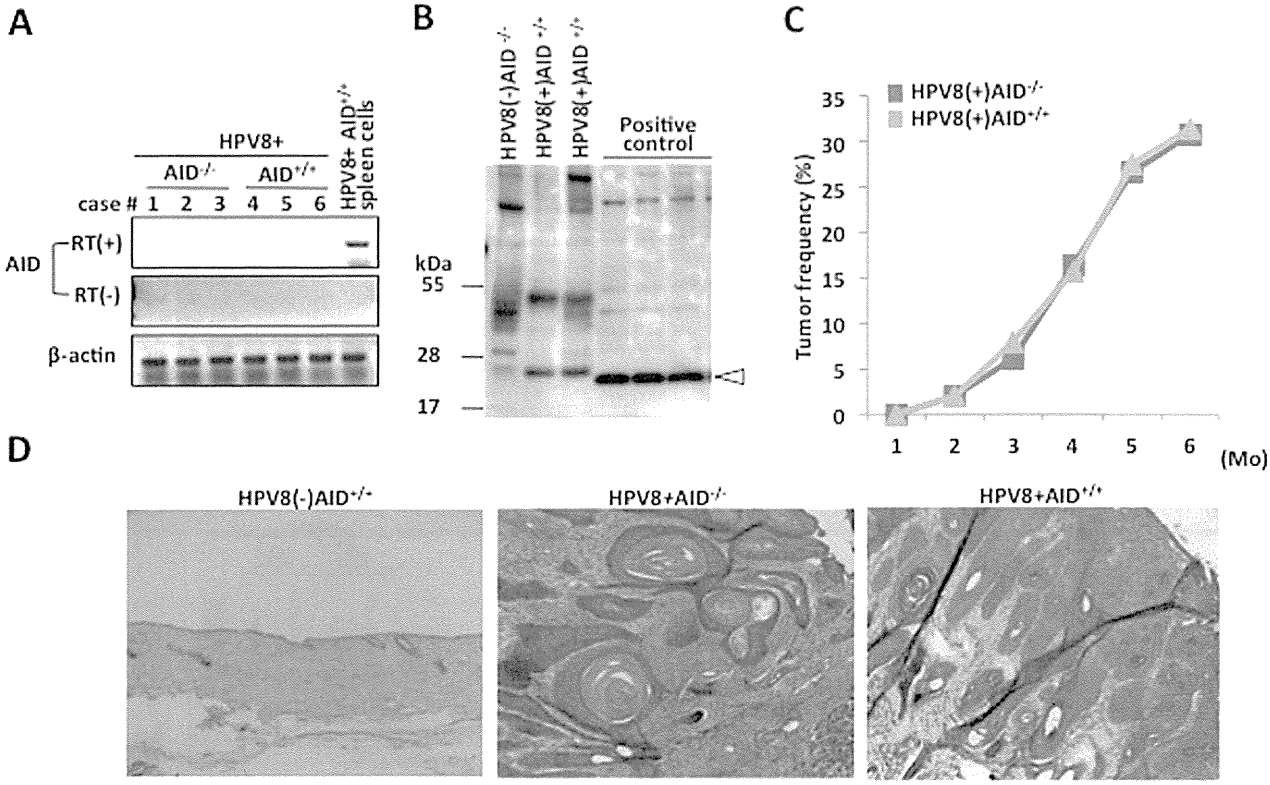

Fig. 5. Cutaneous papilloma in HPV8(+)AID$^{-/-}$ and HPV8(+)AID$^{+/+}$ mice. (A) Representative results of the RT–PCR analysis of AID mRNA in skin tumors of HPV8(+)AID$^{-/-}$ (cases 1, 2, 3) and HPV8(+)AID$^{+/+}$ (cases 4, 5, 6) littermates, and a positive control (naive spleens of HPV8(+)AID$^{+/+}$ mice). The data shown are representative of three independent experiments (n = 9 for each group). (B) Representative results of western blots detecting AID protein in lysates of skin tumors from HPV8(+)AID$^{+/+}$ mice. The negative control was skin tissue from HPV8-Tg negative AID$^{-/-}$, and the positive control was a lysate of spleen cells from HPV8(+)AID$^{+/+}$ mice that was cultured with LPS and IL-4 for 3 days. The arrowhead shows the specific band of AID protein. (C) Papilloma frequency after birth in HPV8(+)AID$^{-/-}$ and HPV8(+)AID$^{+/+}$ mice. (D) H&E staining of skin tissues from HPV8(+)AID$^{+/+}$ and HPV8(+)AID$^{-/-}$ mice.

production with more severe histological phenotypes than the HCV(+)AID$^{-/-}$ mice.

AID is reported to be expressed in HCC and in the surrounding non-cancerous liver tissues (6, 7). In addition, the hepatoma-derived cell lines HepG2, Hep3B and Huh-7 have all been shown to express AID in response to HCV core protein-induced NF-κB signaling (9). It therefore has been assumed that AID is induced in HCV-Tg mice and contributes to liver carcinogenesis. However, AID expression was not detected in HCV core protein-positive hepatocytes, and the low levels of AID transcripts in liver tissues were attributable to infiltrating B cells in this study. The different AID expression levels observed in the present mouse model and HCV-infected patients could be due in part to pathogenic differences between the two systems. HCV-Tg mice lack cirrhotic changes (12, 13), which may be involved in inducing AID expression. In contrast, the natural course of human HCV infection leads to chronic hepatitis development, with bile duct damage and steatosis in the majority of patients (24), and the failure of virus eradication leads to liver cirrhosis and/or HCC (25). In human cases, 80–90% of the HCC develops from cirrhotic liver tissues (21), indicating that chronic inflammatory reactions generally contribute to carcinogenesis.

The involvement of B and T cells in liver injury via autoimmune antibody may be a possible reason for the strong inflammatory response in some part of natural HCV infection cases (26–28). CD81, an HCV-binding molecule, is expressed on the surface of B and T cells and both type of lymphocyte may be infected by HCV (28, 29). HCV infection of B cells causes the development of non-organ-specific auto-antibodies (NOSAs) and cryoglobulinemia (26, 30). In the various NOSAs, some antibodies add auto-antibody-mediated liver injury to viral hepatitis (30). For example, anti-liver/kidney microsomal antibody type 1 (LKM1) and anti-smooth muscle antibody (SMA) are also found in autoimmune hepatitis, and anti-microsomal antibody (AMA) is closely related to primary biliary cirrhosis (31). These liver-targeting antibodies of NOSAs are proposed to be produced based on the mimicry of autoantigens by HCV polyproteins including NS3, 4 and 5 in addition to core proteins (32). In the current HCV-Tg mouse model, auto-antibody-dependent liver injury is less likely because only the core of the HCV polyprotein is expressed and HCV infection in B cells is absent. The absence of this extra-hepatic complication partly explains the reasons why the inflammation is weak in this study compared to natural HCV infection and why AID is not expressed in the hepatocytes of HCV-Tg mouse.

The discrepancy of AID expression between the current animal study and the natural HCV infection could be also due to different regulation of AID expression between mouse and human hepatocytes. The transcriptional regulation of AID expression in B lymphocytes has been extensively examined both *in vitro* and *in vivo* and shown to depend on B-cell-specific and environmental stimulus-specific factors (33). The latter include Stat6 and NF-κb, which are activated by viral infection. AID was activated by transfected HCV core protein responding to the NF-κB signaling pathway (9) in human cell lines; however, NF-κB is not activated in the current HCV-Tg model whereas the upstream TNF-α signal is increased (23). Although the difference in the AID promoter between human and mice is not known, we cannot totally exclude this possibility to explain the different AID expression response.

Although HCV-Tg had weaker inflammatory responses than natural HCV infection, the inflammation observed in HCV(+) $AID^{+/+}$ mice tended to be more severe than that in HCV(+) $AID^{-/-}$ mice. The HCV core protein expression induced infiltration of IHICs including T, B and probably NK cells, and $AID^{+/+}$ B cells enhanced TNF-α production more than $AID^{-/-}$ B cells. The mechanism of TNF-α up-regulation by AID is unknown; however, higher levels of TNF-α production are likely to affect the pathogenesis or prognosis. TNF-α and IL-1β were increased in the whole liver lysates of 16-month-old HCV-Tg mice, as previously reported (23). Clinically, increased TNF-α production from liver-infiltrating monocytes in Non-A, Non-B hepatitis has also been reported (34). Furthermore, TNF-α was shown to activate the AP-1 pathway (23), which promotes cell proliferation (35).

The HCC development without severe 'cirrhotic' findings may be due to carcinogenic properties associated with the HCV core protein, including suppression of apoptosis (by interacting with p53 and pRb), promotion of proliferation (by up-regulating the Wnt/b-catenin and Raf/MAPK pathways) and induction of reactive oxygen species (10, 36).

Stat3 is essential for HPV8-induced skin carcinogenesis (37). The Stat6 and Stat3 DNA recognition motifs are not completely identical, but share partial homology (38). We suspected that HPV8 induces AID through Stat and NF-κB signaling pathways and examined AID's involvement in the HPV8-Tg mouse model. Contrary to our expectation, AID expression was not induced in the HPV8-Tg mouse model, which developed papilloma at a frequency of 30%. Since we observed these mice only up to 6 months before SCC development, we cannot rule out the possibility that AID in the skin squamous cells is induced later to convert papilloma to SCC.

In conclusion, our results suggest that AID may not be essential for either HCV-induced liver carcinogenesis or HPV8-induced papillomagenesis. We were unable to detect AID expression in transgenic cells expressing viral oncogenic proteins in either model, contrary to expectations. These results indicate that the expression of AID is strictly regulated in both hepatocytes and cutaneous keratinocytes at least in the mouse models used here.

Supplementary data

Supplementary data are available at *International Immunology* Online.

Funding

Ministry of Education, Culture, Sports, Science and Technology of Japan Grant-in-Aid for Specially Promoted Research (17002015 to T.H.); Grant-in-Aid for Scientific Research (C) (25440007 to M.K.).

Acknowledgements

We thank Prof. Tsutomu Chiba for helpful discussions, Prof. Hitoshi Nagaoka for useful suggestions, Dr Le Thi Huong for technical assistance and Mrs Mikiyo Nakata for providing HepG2 cells.

References

1 Honjo, T., Kinoshita, K. and Muramatsu, M. 2002. Molecular mechanism of class switch recombination: linkage with somatic hypermutation. *Annu. Rev. Immunol.* 20:165.
2 Nagaoka, H., Tran, T. H., Kobayashi, M., Aida, M. and Honjo, T. 2010. Preventing AID, a physiological mutator, from deleterious activation: regulation of the genomic instability that is associated with antibody diversity. *Int. Immunol.* 22:227.
3 Okazaki, I. M., Hiai, H., Kakazu, N. *et al.* 2003. Constitutive expression of AID leads to tumorigenesis. *J. Exp. Med.* 197:1173.
4 Matsumoto, Y., Marusawa, H., Kinoshita, K. *et al.* 2007. Helicobacter pylori infection triggers aberrant expression of activation-induced cytidine deaminase in gastric epithelium. *Nat. Med.* 13:470.
5 Machida, K., Cheng, K. T., Sung, V. M. *et al.* 2004. Hepatitis C virus induces a mutator phenotype: enhanced mutations of immunoglobulin and protooncogenes. *Proc. Natl Acad. Sci. USA* 101:4262.
6 Kou, T., Marusawa, H., Kinoshita, K. *et al.* 2007. Expression of activation-induced cytidine deaminase in human hepatocytes during hepatocarcinogenesis. *Int. J. Cancer* 120:469.
7 Vartanian, J. P., Henry, M., Marchio, A. *et al.* 2010. Massive APOBEC3 editing of hepatitis B viral DNA in cirrhosis. *PLoS Pathog.* 6:e1000928.
8 Ishikawa, C., Nakachi, S., Senba, M., Sugai, M. and Mori, N. 2011. Activation of AID by human T-cell leukemia virus Tax oncoprotein and the possible role of its constitutive expression in ATL genesis. *Carcinogenesis* 32:110.
9 Endo, Y., Marusawa, H., Kinoshita, K. *et al.* 2007. Expression of activation-induced cytidine deaminase in human hepatocytes via NF-kappaB signaling. *Oncogene* 26:5587.
10 Tsai, W. L. and Chung, R. T. 2010. Viral hepatocarcinogenesis. *Oncogene* 29:2309.
11 McGivern, D. R. and Lemon, S. M. 2011. Virus-specific mechanisms of carcinogenesis in hepatitis C virus associated liver cancer. *Oncogene* 30:1969.
12 Moriya, K., Yotsuyanagi, H., Shintani, Y. *et al.* 1997. Hepatitis C virus core protein induces hepatic steatosis in transgenic mice. *J. Gen. Virol.* 78 (Pt 7):1527.
13 Moriya, K., Fujie, H., Shintani, Y. *et al.* 1998. The core protein of hepatitis C virus induces hepatocellular carcinoma in transgenic mice. *Nat. Med.* 4:1065.
14 Akgül, B., Cooke, J. C. and Storey, A. 2006. HPV-associated skin disease. *J. Pathol.* 208:165.
15 Schaper, I. D., Marcuzzi, G. P., Weissenborn, S. J. *et al.* 2005. Development of skin tumors in mice transgenic for early genes of human papillomavirus type 8. *Cancer Res.* 65:1394.
16 Muramatsu, M., Kinoshita, K., Fagarasan, S., Yamada, S., Shinkai, Y. and Honjo, T. 2000. Class switch recombination and hypermutation require activation-induced cytidine deaminase (AID), a potential RNA editing enzyme. *Cell* 102:553.
17 Qin, H., Suzuki, K., Nakata, M. *et al.* 2011. Activation-induced cytidine deaminase expression in CD4+ T cells is associated with a unique IL-10-producing subset that increases with age. *PLoS ONE* 6:e29141.
18 Kobayashi, M., Aida, M., Nagaoka, H. *et al.* 2009. AID-induced decrease in topoisomerase 1 induces DNA structural alteration

and DNA cleavage for class switch recombination. *Proc. Natl Acad. Sci. USA* 106:22375.
19 Takai, A., Toyoshima, T., Uemura, M. *et al.* 2009. A novel mouse model of hepatocarcinogenesis triggered by AID causing deleterious p53 mutations. *Oncogene* 28:469.
20 Blom, K. G., Qazi, M. R., Matos, J. B., Nelson, B. D., DePierre, J. W. and Abedi-Valugerdi, M. 2009. Isolation of murine intrahepatic immune cells employing a modified procedure for mechanical disruption and functional characterization of the B, T and natural killer T cells obtained. *Clin. Exp. Immunol.* 155:320.
21 Fattovich, G., Stroffolini, T., Zagni, I. and Donato, F. 2004. Hepatocellular carcinoma in cirrhosis: incidence and risk factors. *Gastroenterology* 127(5 Suppl 1):S35.
22 Castello, G., Scala, S., Palmieri, G., Curley, S. A. and Izzo, F. 2010. HCV-related hepatocellular carcinoma: from chronic inflammation to cancer. *Clin. Immunol.* 134:237.
23 Tsutsumi, T., Suzuki, T., Moriya, K. *et al.* 2002. Alteration of intrahepatic cytokine expression and AP-1 activation in transgenic mice expressing hepatitis C virus core protein. *Virology* 304:415.
24 Bach, N., Thung, S. N. and Schaffner, F. 1992. The histological features of chronic hepatitis C and autoimmune chronic hepatitis: a comparative analysis. *Hepatology* 15:572.
25 World Health Organization (WHO). 2013. *Hepatitic C fact Sheet* No 164. Media Centre.
26 Sansonno, D., Tucci, F. A., Lauletta, G. *et al.* 2007. Hepatitis C virus productive infection in mononuclear cells from patients with cryoglobulinaemia. *Clin. Exp. Immunol.* 147:241.
27 Himoto, T. and Nishioka, M. 2008. Autoantibodies in hepatits C virus-related chronic liver disease. *Hepatitis Monthly* 8:295.
28 Deng, J., Dekruyff, R. H., Freeman, G. J., Umetsu, D. T. and Levy, S. 2002. Critical role of CD81 in cognate T-B cell interactions leading to Th2 responses. *Int. Immunol.* 14:513.
29 Zhang, J., Randall, G., Higginbottom, A., Monk, P., Rice, C. M. and McKeating, J. A. 2004. CD81 is required for hepatitis C virus glycoprotein-mediated viral infection. *J. Virol.* 78:1448.
30 Bogdanos, D. P., Mieli-Vergani, G. and Vergani, D. 2005. Non-organ-specific autoantibodies in hepatitis C virus infection: do they matter? *Clin. Infect. Dis.* 40:508.
31 Zeman, M. V. and Hirschfield, G. M. 2010. Autoantibodies and liver disease: uses and abuses. *Can. J. Gastroenterol.* 24:225.
32 Gregorio, G. V., Choudhuri, K., Ma, Y. *et al.* 2003. Mimicry between the hepatitis C virus polyprotein and antigenic targets of nuclear and smooth muscle antibodies in chronic hepatitis C virus infection. *Clin. Exp. Immunol.* 133:404.
33 Tran, T. H., Nakata, M., Suzuki, K. *et al.* 2010. B cell-specific and stimulation-responsive enhancers derepress Aicda by overcoming the effects of silencers. *Nat. Immunol.* 11:148.
34 Yoshioka, K., Kakumu, S., Arao, M. *et al.* 1990. Immunohistochemical studies of intrahepatic tumour necrosis factor alpha in chronic liver disease. *J. Clin. Pathol.* 43:298.
35 Shaulian, E. and Karin, M. 2001. AP-1 in cell proliferation and survival. *Oncogene* 20:2390.
36 Liang, T. J. and Heller, T. 2004. Pathogenesis of hepatitis C-associated hepatocellular carcinoma. *Gastroenterology* 127(5 Suppl 1):S62.
37 De Andrea, M., Rittà, M., Landini, M. M. *et al.* 2010. Keratinocyte-specific stat3 heterozygosity impairs development of skin tumors in human papillomavirus 8 transgenic mice. *Cancer Res.* 70:7938.
38 Ehret, G. B., Reichenbach, P., Schindler, U. *et al.* 2001. DNA binding specificity of different STAT proteins. Comparison of in vitro specificity with natural target sites. *J. Biol. Chem.* 276:6675.